Geoscience BC Report 2016-19

Mud Volcanoes in the Purcell Basin and Their Relevance to Middle Proterozoic Massive-Sulphide Ag-Pb-Zn Deposits, Southeastern British Columbia

Sean Kennedy
Trygve Höy

Geoscience BC

When using information from this publication in other publications or presentations, due acknowledgment should be given to Geoscience BC. The following reference format is recommended:

Kennedy, S. and Höy, T. (2015): Mud Volcanoes in the Purcell Basin and Their Relevance to Middle Proterozoic Massive Sulphide Ag-Pb-Zn Deposits; Geoscience BC, Report 2016-19, 55 p.

NTS grid: NTS 082F/01, /08, /09, 082G/04, /05, /12

Keywords: SEEK, geology, geochemistry, Purcell Basin, mud volcanism, massive sulphide

Author addresses:
Sean Kennedy
Consultant
Kimberley, BC
E-mail: js_kenn@shaw.ca

Trygve Höy
Consultant
Sooke, BC
E-mail: thoy@shaw.ca

Published by:
Geoscience BC
Suite 1101 – 750 West Pender Street
Vancouver BC
V6C 2T7
Phone: (604) 662-4147
E-mail:info@geosciencebc.com
Website: www.geosciencebc.com

Cover photo: Crosscutting, tourmalinized mud-volcano pipe at the Pakk property.

Geoscience BC is an independent, non-profit organization that generates earth science in collaboration with First Nations, local communities, government, academia and the resource sector. Our independent earth science enables informed resource management decisions and attracts investment and jobs. Geoscience BC gratefully acknowledges the financial support of the Province of British Columbia.

Abstract

This paper details the results of a geological and geochemical study that was undertaken in the summer of 2014 to determine the base metal potential of sedimentary fragmental rocks in the Purcell Basin of southeastern British Columbia.

Fragmental rocks related to mud/sediment volcanism and venting were developed episodically during deposition of the Aldridge Formation and may be genetically related to the giant Sullivan Pb-Zn-Ag deposit at Kimberley. The goal of this project, funded as part of Geoscience BC's SEEK program, was to determine if it was possible to differentiate the favourability of various fragmental complexes to host base metal mineralization, or vector within the complexes to areas of higher mineralization potential, by cataloguing fragmental facies, defining controlling structures and alteration zones, and determining geochemical signatures as they may relate to the venting process. Five previously identified fragmental occurrences were selected as study areas based on access, current level of exploration interest, and stratigraphic location. Geological mapping of fragmental alteration assemblages was shown to be an effective tool for evaluating fragmental facies and their potential for base metal mineralization. Additionally, mapping of mud/sediment volcano facies and structural trends was shown to be a useful tool for interpreting the local sedimentary environment. Geochemical variations between sample sites were identified and further whole rock and trace element analyses should help identify the geochemical signature of mineralized fragmental complexes.

Table of Contents

Tables

Figures

Introduction

Sedimentary fragmental rocks associated with episodic mud/sediment volcanism and venting processes in the Aldridge Formation of the Purcell Basin of southeastern British Columbia have been described and categorized in previous studies including; Höy, 1993, Britton et al, 1994, Höy et al, 1994, Brown et al, 1998, Anderson et al, 2000, Turner et al., 2000a, Turner et al., 2000b, and Lydon, 2008. Sedimentary fragmental rocks include rounded to angular clast-rich lithologies and breccias that are interpreted to have formed due to sediment fluidization and mud/sediment volcanism (Höy, 1993, Anderson, et al, 2000, Turner et al., 2000b). Many are spatially associated with base metal sulphide deposits hosted within the Aldridge Formation including the world class Sullivan Pb-Zn-Ag SEDEX deposit. Exploration within the Purcell Basin has largely focused on deep drilling to evaluate the Lower Aldridge-Middle Aldridge contact, the stratigraphic interval which hosts the Sullivan deposit (Sullivan-time). Sedimentary fragmental rocks, sometimes 1000s of meters above this interval, have been used as vectors by explorationists for targeting deep drilling, while only a limited amount of drilling has been focused on evaluating the shallower targets directly associated with these fragmental rocks.

The aim of the 2014 program was to map fragmental complex facies, geometry and alteration and develop guidelines to identify their association with base metal systems. Intervals above the strata which hosts the Sullivan deposit were selected for study as they have remained largely underexplored by industry. Geochemical analysis of lithologies and alteration zones associated with the fragmental facies were undertaken to differentiate barren and mineralized systems and to establish a geochemistry database.

The area encompassing the Purcell Basin and equivalent Belt Basin in the United States (collectively referred to as the Belt-Purcell Basin) is an important metallogenic province covering approximately 200,000 km^2 (Figure 1). The Purcell Basin encompasses approximately one fifth of the entire Belt-Purcell Basin (Lydon, 2008). The largest base metal deposit in the Purcell Basin was the Sullivan Mine (closed in 2001) which initially contained over 160 million tons of ore at 6.5% Pb, 5.6% Zn, and 67 g/t Ag. Other important metal deposits within the Belt-Purcell Basin include;

- the world-class Coeur d'Alene Ag-Pb-Zn vein district,
- the large stratabound Cu-Ag deposits of northwest Montana, and
- the porphyry/epithermal Cu-Ag-Au deposits at Butte, Montana.

Despite the metal endowment of the basin it remains an underexplored region. Our study selected five occurrences of fragmental facies within the Aldridge Formation stratigraphically above Sullivan-time that had been previously identified by industry and compiled onto the regional 1:50,000 Geological Survey of Canada Open File maps OF6302, OF6303, OF6304, and OF6305 (Brown and Macleod, 2011, Brown et al., a, 2011, Brown et al., b, 2011, Brown et al., c, 2011). While two of the study areas (Rise and Pakk) had been drill-tested, detailed surface mapping of the fragmental units and geochemical analysis were lacking for all of the sites.

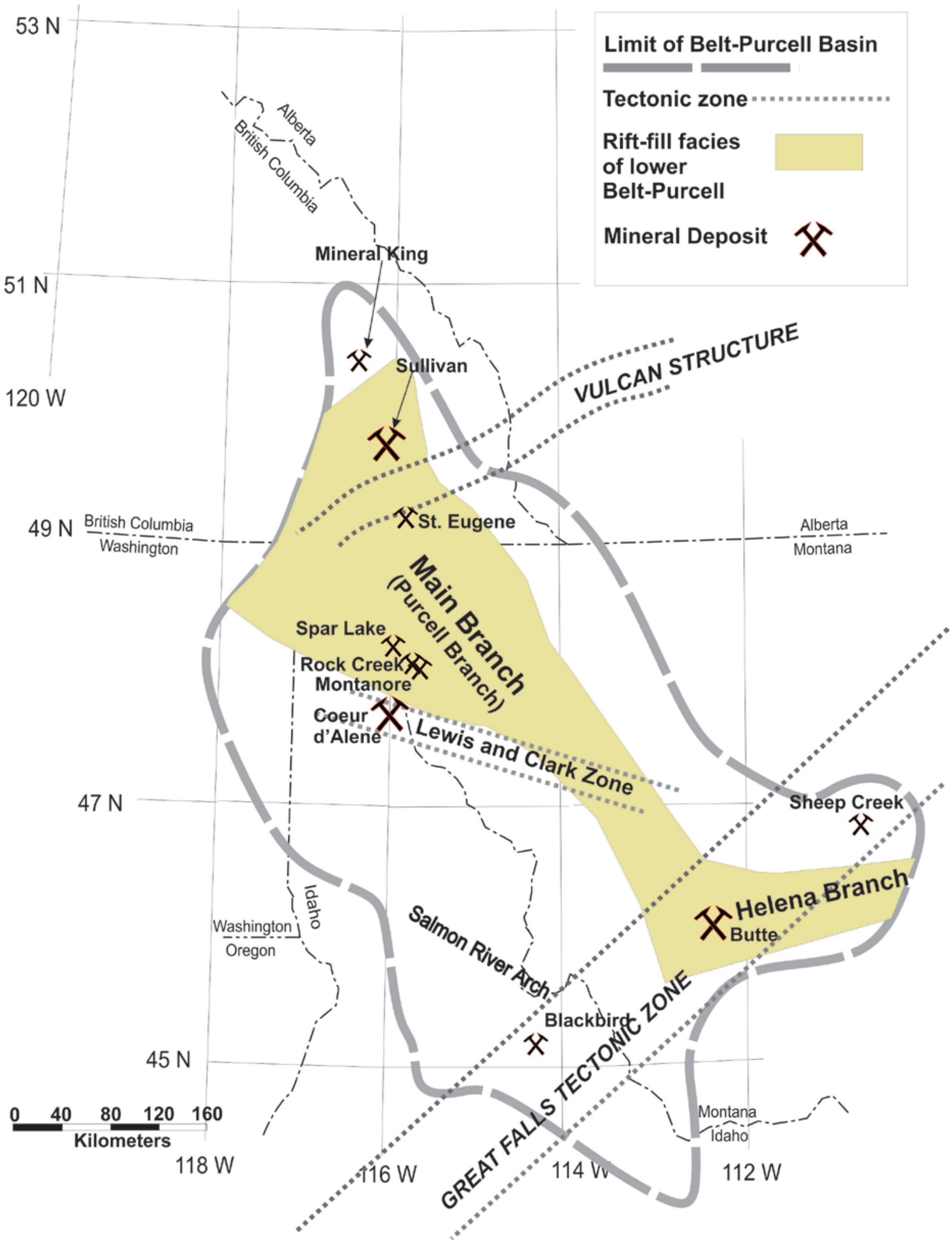

Figure 1. *Geographical limit of Belt-Purcell basin with important mineral deposits and tectonic features (after Price et al., 2000 and Lydon, 2008).*

Regional Geology

Stratigraphy

The study area is underlain by the Mesoproterozoic Purcell Supergroup, an approximately 20 km thick package of clastic, carbonate and lesser volcanic rocks (Höy, 1993) deposited within a branching intracontinental rift of an Archean and Paleoproterozoic craton (Höy, 1993, Price et al., 2000). The Main Branch of the Belt-Purcell Basin, also known as the Purcell Branch, that formed along a northwest-trending axis (Lydon, 2008), underlies the study area (Figure. 1).

Within the Purcell Supergroup is the Aldridge Formation which can be subdivided into Lower, Middle, and Upper members;

- The Lower Aldridge is composed of rusty weathering thin to medium-bedded quartz wacke and argillite deposited as distal turbidites, intercalated with numerous gabbro sills. The base of the Lower Aldridge is not exposed, however seismic imaging indicates the sediment-sill complex is upwards of 9 km thick (Cook and van der Velden, 1995).
- The overlying Middle Aldridge comprises approximately 2500 m of grey to rusty, medium to thick-bedded turbidites and lesser argillite. At least twenty known time-stratigraphic marker horizons occur in the Middle Aldridge. These rocks display laminated, barcode-like intervals, commonly within thicker sequences of rusty, pyrrhotitic, finely-laminated siltstone, wacke, and argillite. Alternating mm- to cm-scale light and dark laminae composed of quartz, feldspar, biotite, muscovite, and graphite form the barcode-like banding diagnostic of these horizons. The distinctive varved laminae within marker units can be correlated with precision over regional distances and provide stratigraphic control in the dominantly turbiditic environment.
- The Upper Aldridge comprises approximately 300 m of platy and rusty sulphidic argillite (Höy, 1993).

Overlying the Aldridge is the shallow-water, clastic Creston Formation and carbonate-rich Kitchener Formation. Above the Kitchener are the Nicol Creek basalts and overlying shallow-water to sub-aerial clastic rocks of the Upper Purcell Supergroup.

Tectonic and Metamorphic History

Rocks of the Purcell Supergroup are exposed in the core of the Purcell Anticlinorium, a large north-trending open fold complex cut by numerous northeast-trending transverse faults including the Moyie/Dibble and St. Mary/Boulder Creek faults (Höy, 1993). These faults bound the Vulcan Low, a major transverse zone of basement structures that have been re-activated intermittently from the Archean to the Cenozoic (McMechan, 2010). The earliest tectonic event in the Purcell Basin is recorded by block-faulting related to extension during Aldridge Formation deposition as illustrated by major facies changes in Aldridge Formation sediments along the Boulder Creek fault (Höy, 1993), additionally, growth structures along, and parallel to the basin margin were active during this period. The intrusion of the basaltic Moyie suite occurred during this early extensional period (Höy, 1993). Extensional tectonism waned during deposition of the Upper Aldridge but was renewed and continued throughout the formation of the Nicol Creek basaltic lavas and Upper Purcell Supergroup rocks (Sheppard/Gateway/Dutch Creek Formations). Paleozoic faulting is shown along the antecedent Moyie-Dibble Creek fault during the Early Cambrian and late Devonian when rocks were uplifted to the south and down-dropped to the northwest (Lydon, 2008). At least three periods of regional metamorphism and deformation have occurred in the Purcell Basin; the East Kootenay Orogeny (1350-1300 Ma), observed in burial metamorphism, the Goat River Orogeny (900-800 Ma), marked by uplift, block-faulting and metamorphism at the onset of the deposition of the Windermere Supergroup, and the late Mesozoic/early Cenozoic Laramide event that compressed and displaced the Purcell Supergroup northeastward along re-activated transverse basement structures (Price et al., 2000, Lydon, 2008). This event created large-scale, north-plunging folds and the emplacement of a suite of mid-Cretaceous granitic bodies (Höy, 1993). Later relaxation along these structures has led to some faults showing net normal displacement (Höy, 1993). The highest metamorphic grade in the study area is upper greenschist (Höy, 1993).

Mineralization

The Belt-Purcell Basin is a major lead-zinc-copper-silver-gold metallogenic province which hosts a range of deposits that formed during the Mesoproterozoic and later Mesozoic (see Tables 1 and 2; Lydon, 2008). Mesoproterozoic deposits within the Belt-Purcell have been subdivided into six types; SEDEX deposits, Besshi-type deposits, vent complex/feeder pipe deposits, stratabound disseminated sulphide deposits (Cu-Ag, Pb-Zn-Ag), and vein deposits (Lydon, 2008).

The Belt-Purcell has seen production from four major mining districts; Sullivan (Pb-Zn-Ag, SEDEX), Coeur d'Alene, Idaho (Pb-Zn-Ag veins), Spar Lake, Montana (Cu-Ag, sediment-hosted), and Butte, Montana (Cu-Zn-Ag-Au, porphyry/epithermal). The area has also produced significant amounts of placer gold, particularly in the Cranbrook area.

The Purcell Basin (the Canadian portion of the Belt-Purcell Basin) covers approximately 40,000 km² and is most well known for hosting the Sullivan deposit, a world-class Pb-Zn-Ag SEDEX deposit. Sullivan is considered to be a syngenetic seafloor deposit which occurs just below the contact of the Lower and Middle Aldridge Formations (see Figures 2 and 3, Lydon, 2008).

Table 1. *Significant Mesoproterozoic deposits within the Belt-Purcell Basin (after Lydon, 2008).*

Name	Deposit Type	Cu%	Co %	Zn %	Pb %	Ag g/t	Au g/t	Tonnes
Kootenay King	SEDEX			15.6	5.35	67		13,000
North Star	SEDEX			6.12	35.5	673		61,000
Sullivan	SEDEX			5.86	6.08	67		161,970,000
Sheep Creek Lower Zone	SEDEX	6						1,800,000
Sheep Creek Upper Zone	SEDEX	2.5	0.1					4,500,000
Blackbird	Besshi	1.5	0.6					960,099
Stemwinder	Vent Complex			15.6	3.7	76		25,000
Spar Lake	Stratabound Cu-Ag	0.76				54		58,000,000
Rock Creek	Stratabound Cu-Ag	0.68				51		143,700,000
Montanore	Stratabound Cu-Ag	0.74				60		134,500,000
Coeur d'Alene District	Vein			2.62	6.66	313		109,496,626
St. Eugene	Vein			0.98	7.66	124	0.05	1,475,266
Vine	Vein			2.4	4.6	52	1.8	547,000

Table 2. *Production from the major mining districts within the Belt-Purcell Basin (after Lydon, 2007).*

Name	Deposit Type	Au (tonnes)	Ag (tonnes)	Cu (tonnes)	Pb (tonnes)	Zn (tonnes)
Sullivan	SEDEX		9,264		8,412,077	7,944,446
Coeur d'Alene District	Veins		35,600		7,400,000	2,900,000
Spar Lake	Stratabound Cu-Ag		138	26,215		
Butte District	Porphyry epithermal	87	22,600	9,700,000	387,389	2,500,000

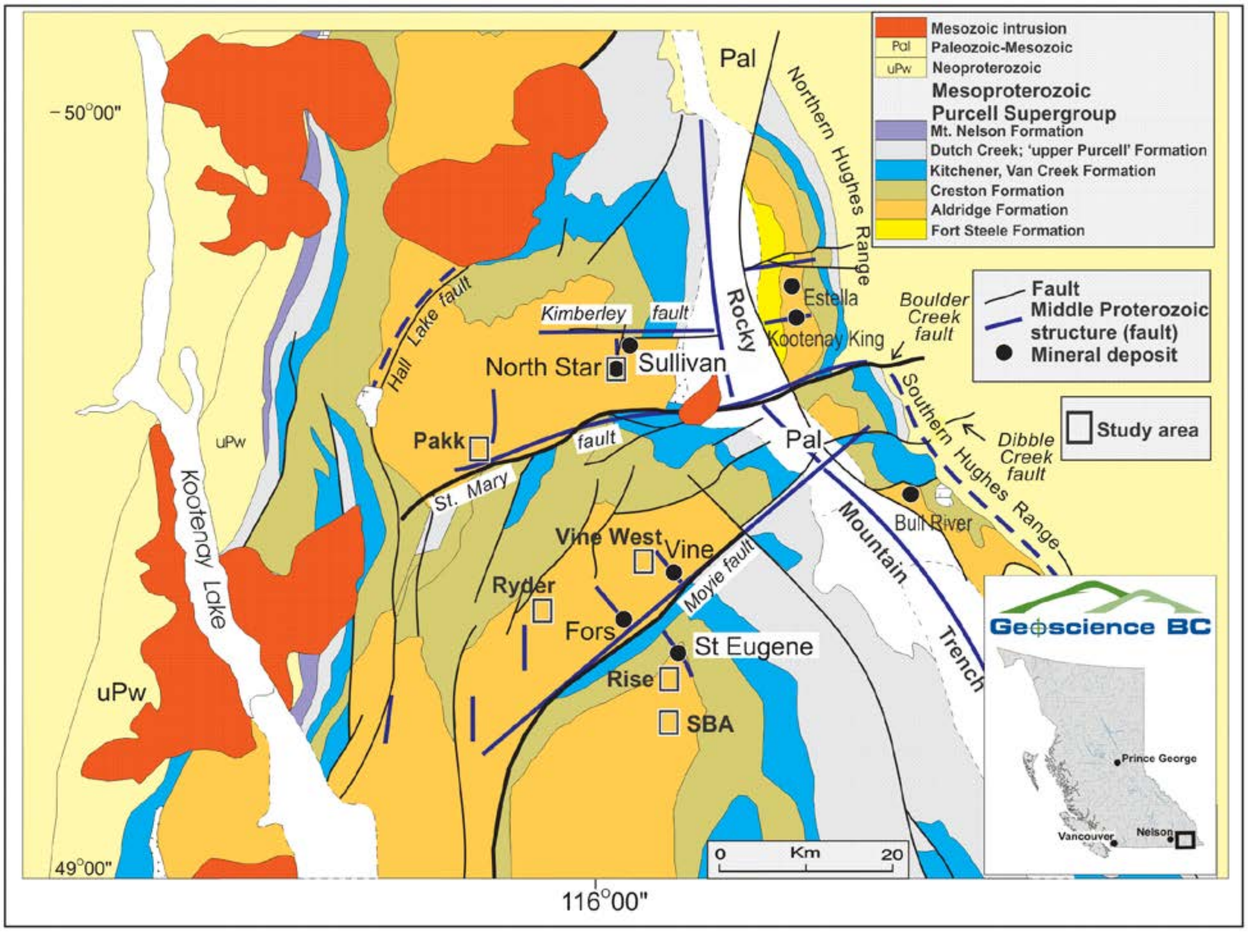

Figure 2. *Regional geology of the Purcell Supergroup showing important mineral deposits; black boxes show 2014 study areas (after Lydon, 2008).*

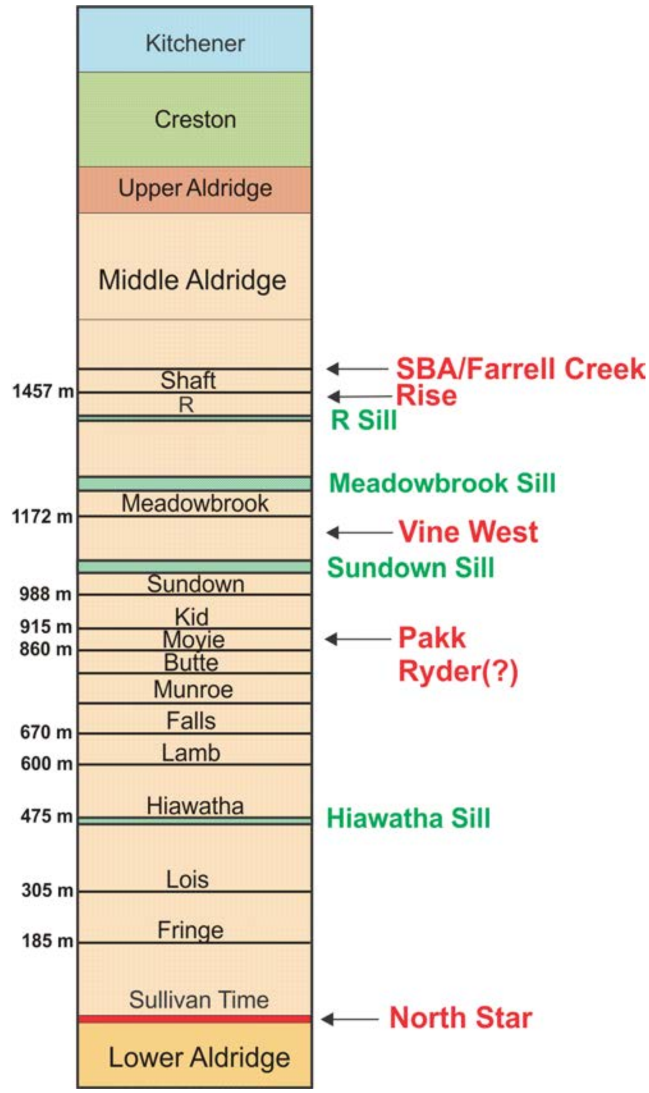

Figure 3. *Generalized stratigraphic column of the Middle Aldridge Formation showing the major regional marker horizons and the idealized depth to the Lower Aldridge contact. Regional Moyie sills are shown in green and stratigraphic position of 2014 study areas are shown with red text.(after Brown et al, 2011).*

Sedimentary Volcanism and Hydrothermal Vents

Mud, or sedimentary, volcanism refers to the formation of various geological structures due to the expulsion of clay and silt-rich fluidized sediment at the surface (Dimitrov, 2002). Submarine mud volcanoes form seafloor structures similar to magmatic volcanoes and are effective pathways for the venting of gas and fluid from the crust. They form in both passive and active margins and are generally thought to be related to mud diapirism, the process whereby clay-rich sediment, hosted within a parent bed, rises as a buoyant mass through denser stratigraphy (Knopf, 2002). Whether diapirs breech surface to form mud volcanoes depends on the amount of pore-fluid pressure within the diapir and the lithostatic pressure of the overlying pile. Mud volcanoes may also occur where a mud diatreme, not necessarily related to a diapir, is forcefully injected into overlying sediment and breeches the surface (Knopf, 2002). Mud diapirs may rise simply due to a density inversion (Knopf, 2002); however, high pore-fluid pressure within the sedimentary pile can enhance the process. Conversely, the formation of a mud diatreme *requires* high pore-fluid pressure (Dimitrov, 2002). Pore-fluid pressure can be increased tectonically by over-pressuring sediments in compressive regimes and by rapid sediment loading in extensional environments. Fluids derived from mineral dehydration, or transported hydrothermal fluids or brines, can increase pore-fluid pressure within a parent stratigraphy. High pore-fluid pressure can also be enhanced by gas generation from either, or a combination of mantle degassing, igneous degassing, and or hydrocarbon formation (Knopf, 2002). If the pore-fluid pressure is high enough within the system various triggers, including seismic disturbance or faulting, may force the liquefaction of a parent bed and form a diatreme (Dimitrov, 2002).

Mud and sediment volcanism was associated with ancient hydrothermal vent systems in the Møre and Vøring basins in the northeast Atlantic and in the Karoo Basin in South Africa where the volcanism forms basinal piercement structures related to syn-depositional magmatism (Jamtviet et al., 2004: Planke et al., 2005). Hydrothermal fluids generated during the emplacement of large volumes of mafic sills within unconsolidated sediments in the Møre, Vøring, and Karoo basins are thought to have created high enough pore-fluid pressure to form sedimentary diatremes and associated mud volcano deposits. Seismic data from the northeast Atlantic has shown that conduit zones related to hydrothermal vent systems can reach depths of 8 km with the upper portion of the vent complex expressing itself as a mud-volcano (Planke et al., 2005). Recent work has also demonstrated that these systems can operate as effective conduits for migrating gas and fluid long after the original venting process has stopped creating carbonate and methane deposits in the hanging wall of ancient vent sites (Svensen et al., 2003).

A generalized model for hydrothermal venting and mud volcanism related to syn-sedimentary intrusions within the Møre, Vøring, and Karoo basins includes: high-level sill emplacement within unconsolidated sediments, boiling of pore waters, increased pore-fluid pressure, and eventual expulsion of hydrothermal fluids, gas, and remobilized sediment at surface creating a mud or sediment volcano and hydrothermal vent (Jamtveit et al., 2004).

Fragmental Rock Facies Associated With Hydrothermal Vents in the Purcell Basin

Sedimentary fragmental rocks within the Aldridge Formation are considered to have formed as the result of sedimentary volcanism and hydrothermal venting caused by basinal dewatering (Anderson et al., 2000). A mud volcano/hydrothermal vent model for the Purcell Basin, similar to the model from the Møre, Vøring, and Karoo Basins, identifies the intrusion of high-level Moyie sills and dykes into unconsolidated sediments as a principal driver of the mud volcano/hydrothermal vent process, and the eventual formation of fragmental rock facies (Höy, 1993, Anderson et al., 2000).

Fragmental units are of considerable importance for mineral exploration as they are genetically related to the Sullivan deposit, forming both the sub-basin that hosts the deposit and the breccia/feeder zone which underlies the deposit (Lydon, 2000, Turner et al., 2000, Ransom et al., 2000). Fragmental units are also associated with many other massive sulphide deposits and base metal occurrences in the Purcell Basin (Anderson and Höy, 2000).

Sedimentary fragmental rocks within the Purcell Basin occur at different stratigraphic intervals primarily within the Lower and Middle Aldridge Formations and are associated with many of the base metal sulphide deposits in the region. Fragmental units are structurally controlled, occurring along rift-parallel faults, and at the intersection of rift-parallel and transverse structures (Anderson et al., 2000). They are characterized by angular to sub-rounded sedimentary clasts within a homogenous matrix that is compositionally similar to the Aldridge Formation host rock. Previous studies have divided fragmental rocks into different facies based on their relationship to their host rock (Höy, 1993, Brown et al., 1997, Anderson et al., 2000). These sub-divisions include four facies:

- discordant
- vent proximal
- debris flow
- sill concordant

Discordant sedimentary fragmentals cut bedding at high angles, are typically localized along fault zones, and can be clast to matrix-dominated. They form km-scale linear clastic dykes, pipe-like bodies that are round to elliptical in surface plan, or infill small-scale irregular fractures. Clast transportation is indicated by clast roundness and lithological variation of clasts from the sedimentary host sequence. Clasts range from mm- to dm- scale and show some alignment. Discordant sedimentary fragmentals have been shown to be vertically continuous over hundreds of meters (Anderson and Höy, 2000) and are effective pathways for focusing and channeling potentially mineralizing fluids.

Vent proximal fragmental facies are seafloor deposits formed by sediment extrusion. They are clast- to matrix-rich, form mound deposits or fill caldera-like depressions and are related to discordant feeder sedimentary breccias. They are typically fault controlled and form elongate elliptical structures that can range from tens of meters to kilometers in length and have been shown to reach thicknesses over 50 m (Anderson and Höy, 2000).

Debris flow deposits form as a result of the collapse of slopes along vent proximal mounds or along the walls of caldera-type vent proximal depressions. Debris flows deposits help identify third order basins. They are formed by slope instability and failure along bounding extensional structures coupled with sediment extrusion (Ransom et al., 2000). These deposits can be found laterally for kilometers from the vent site and are characterized by soft sediment deformation including; slumped and folded beds, rip-up clasts, and homogenized sediments. Both vent proximal and debris flow deposits have been demonstrated to stack over hundreds of meters of stratigraphy above active discordant feeder zones.

Sill concordant fragmental facies in the Aldridge Formation are laterally extensive and form along the contacts of some Moyie sills. They consist of homogenized coarse, sandy to pebbly sediments, convoluted relict bedding, and locally incorporate gabbroic clasts. They are considered to have formed as a result of boiling of pore-fluids during the emplacement of high-level sills in wet sediments (Höy, 1993) and may be related to stratigraphically higher mud volcano deposits (Anderson et al., 2000). Sill concordant facies were not dealt with in this study.

Mud volcanism in the Purcell Basin developed mainly during deposition of the Aldridge Formation, when prevailing conditions included extension, rapid sediment loading, and coeval magmatism. High pore-fluid pressure could be related to the presence of formational brines, sediment compaction due to loading, mineral dehydration, boiling of pore waters by high-level intrusions and gas generation and the combination of these factors could have caused over-pressuring within the sediment pile. Sudden seismic events might have triggered the release of over-pressured units into fluidized diatremes transporting sediment, fluid, and gas along pre-existing faults. Upon breaching the surface at a vent site, remobilized sedimentary clasts and liquefied sediment would have extruded onto the seafloor forming mud volcano deposits. Cross strata permeability, provided by mud volcano diatremes, would have allowed the over-pressured formational brines and subsequent fluids to escape. Ore deposition is envisaged where metal-bearing fluids were focused and vented into a suitable depositional setting or where later mineralizing fluids were focused into pre-existing diatremes replacing suitable horizons as well as forming discordant massive sulphides (see Figure 4).

Re-activation of Paleoproterozoic faults defined by diatreme and mud-volcano deposits has occurred throughout the history of the Purcell Supergroup. Mesoproterozoic massive sulphide veins, like the St. Eugene and Vine deposits formed within structural zones that host mud volcano deposits. Gold veins associated with Laramide events have also been demonstrated to occur within the same structural zones as mud-volcanoes, indicating that these structures continued to act as foci for mineralization long after sedimentation.

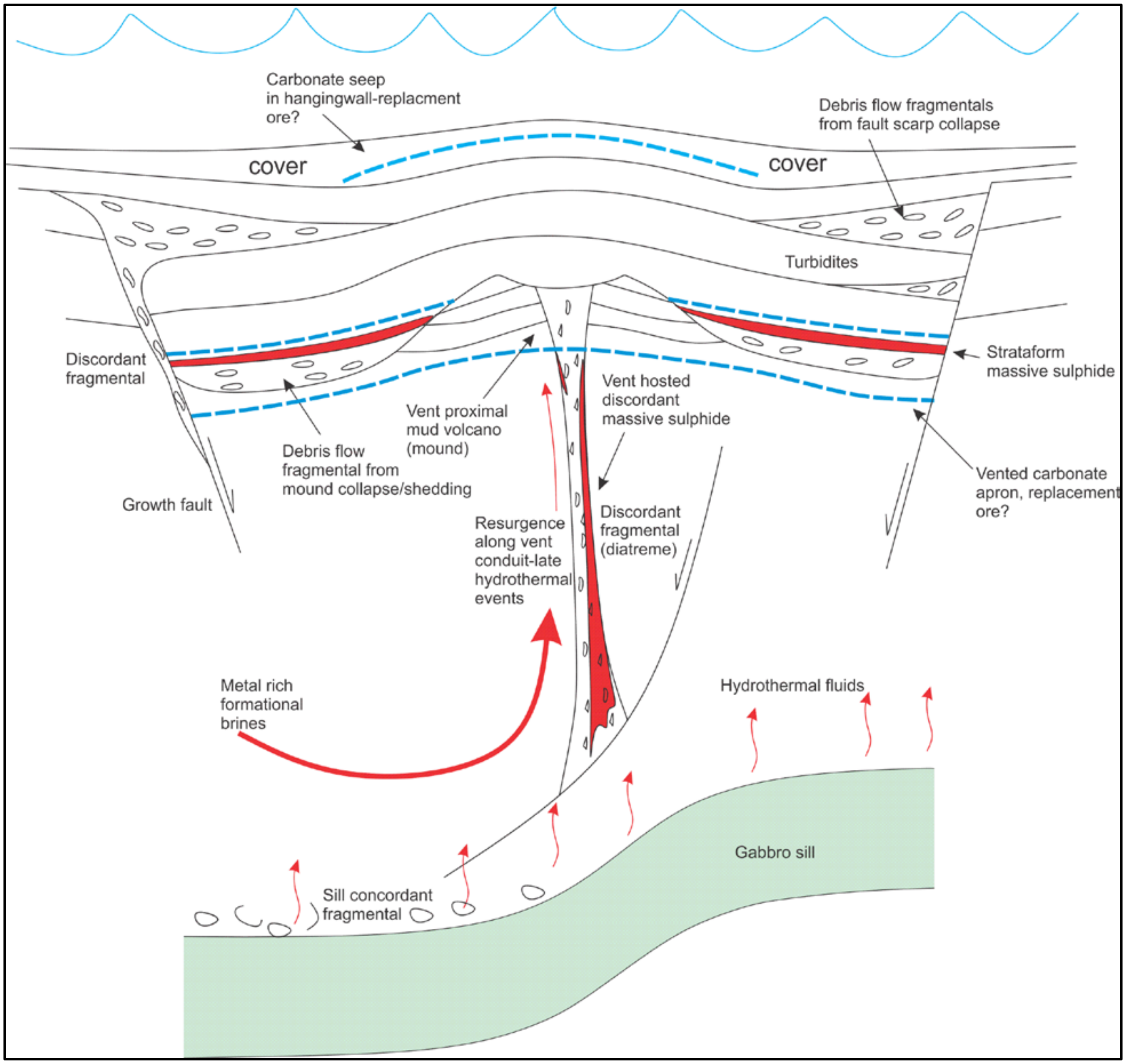

Figure 4. *Conceptual model of an Aldridge Formation mud volcano vent system (after Höy, 1993, Anderson et al., 2000 and Jamtviet et al., 2004).*

Study Plan and Methods

Five study areas (Pakk, Ryder, Rise, SBA, and Vine West) were selected for the project based on; exploration history, current level of exploration activity, and location. The regional 1:50,000 scale government geology maps, which show many fragmental units within the Purcell Basin, were instrumental in determining potential study sites. Additional discussions with local explorationists and the author's local knowledge helped the selection process. The chosen sites are all located within approximately1900 km^2 (Figure 1) and occur at different stratigraphic levels primarily within the upper half of the Middle Aldridge Formation (Figure 2).

Mapping

Field work focused on identifying fragmental unit contact relationships, mapping fragmental unit geometries, distribution of facies, and types and styles of alteration/mineralization. Alteration suites/minerals associated with Aldridge Formation fragmental units described by Britton et al. (1994), and Turner et al., (2000b) were used as guidelines when mapping (see Table 3). As noted by Britton et al. (1994) alteration minerals associated with fragmental units are described using their current metamorphic mineralogy and that the precursor mineral formed from the original hydrothermal fluid is likely not the same mineral as that which was formed during later metamorphism.

Geochemistry

Rock grab samples collected from various alteration zones and lithologies were analyzed by Bureau Veritas of Vancouver using the 1DX 36-element ICP-MS analysis (30 g sample), which was chosen as most early stage exploration projects use a similar package. A study of the Aldridge-equivalent Prichard Formation in the Coeur d'Alene district of Idaho and Montana (Gott et al., 1980) and geochemical data from Cominco (Anderson and Höy, 2000) provided background values for certain elements in Aldridge Formation sedimentary and fragmental rocks (Table 4).

Deliverables

Final deliverables for this project include the maps published in this report, rock geochemical data from 80 grab samples, a poster displayed at Roundup 2015 in Vancouver, and a petrographic report of 10 samples from fragmental complexes collected during the program.

Table 3. *Alteration minerals associated with mud/sediment volcanoes in the Purcell Basin.*

Alteration Mineral	Mode of occurrence
Actinolite/tremolite	Replacement of precursor rock, fibrous masses/clots, veinlets, mineral coatings
Albite (plagioclase)	Replacement of precursor rock, mineral overgrowths?
Biotite	Disseminated flakes, veinlets, patches
Carbonate	Veinlets, clots
Chlorite	Disseminated flakes, patches, veinlets
Garnet	Porphyroblastic
Sericite	Replacement of precursor rock, flakes, patches
Silicification	Replacement of precursor rock, veins
Tourmaline	Replacement of precursor rock, disseminated acicular needles
Iron Sulphides	Veinlets, disseminations, clots

Table 4. *Background values of selected elements in ppm from the Aldridge (Prichard) Formation (Coeur d'Alene district) and from Aldridge Formation sedimentary rocks and fragmental rock facies.*

Coeur d'Alene District		
Element	>75th percentile in ppm	>90th percentile in ppm
As	21	28
Ba	828	1,090
Cu	38	69
Pb	55	125
Mn	475	1083
Ni	17	29
Sb	4.2	7.8
Zn	90	138
Cominco Data	Aldridge sediments	Fragmentals
As	10	20
Cu	26	21
Pb	32	14
Zn	100	50

2014 Study Areas

North Star

Location

North Star hill (Figure 5) is situated along the southern extension of the Sullivan graben (Sullivan corridor) near UTM 570,500 and 5,504,000 (Figure 2) and hosts both vein and SEDEX lead-zinc-silver mineralization (Turner et al, 2000). It is immediately west of the city of Kimberley and is the location of the Kimberley Alpine Resort.

Geology

The geology of the Sullivan graben at North Star hill has been described in detail by previous workers (Turner et al., 2000a, Lydon et al., 2008). The graben is a north-south trending series of syn-sedimentary fault-bound basins approximately 13 km long by 4 km wide (Lydon, 2008). The graben system is defined by conglomeratic deposits up to 300 m thick that are overlain by the Sullivan Horizon, a regionally conspicuous, black, laminated mudstone which occurs at the contact between the Lower and Middle Aldridge Formation (Lydon, 2008). The graben system hosts extensive sulphide vein mineralization, widespread alteration and gabbroic intrusions (Turner et al., 2000a). Clastic dykes and thick accumulations of conglomeratic rock within the graben are considered to have formed as a result of mud volcanism and slope failure (Turner et al., 2000a, Lydon, 2008). Stratiform massive sulphide mineralization (Po-Pb-Zn-Ag) within the graben at the Sullivan and North Star deposits occurs at the top of the conglomeratic units indicating mineralization was related to the waning of the mud volcano system (Turner et al., 2000a).

Sampling

A suite of 13 rock grab samples of altered sulphidic, thin-bedded quartzite, siltstone, argillite and fragmental rocks with no obvious base metal mineralization were collected from below the Sullivan Horizon within the Sullivan graben at North Star hill (Figure 6). These samples were analysed by Bureau Veritas in Vancouver to provide baseline analyses for geochemical comparisons with the study areas.

Results from these samples (Table 5) show elevated average values for Pb (192 ppm), Zn 162 ppm), Cu (34 ppm), and As (21.5 ppm) in comparison to Aldridge Formation rocks (see Table 4).

***Figure 5**. Looking west towards North Star hill (Kimberley Alpine Resort).*

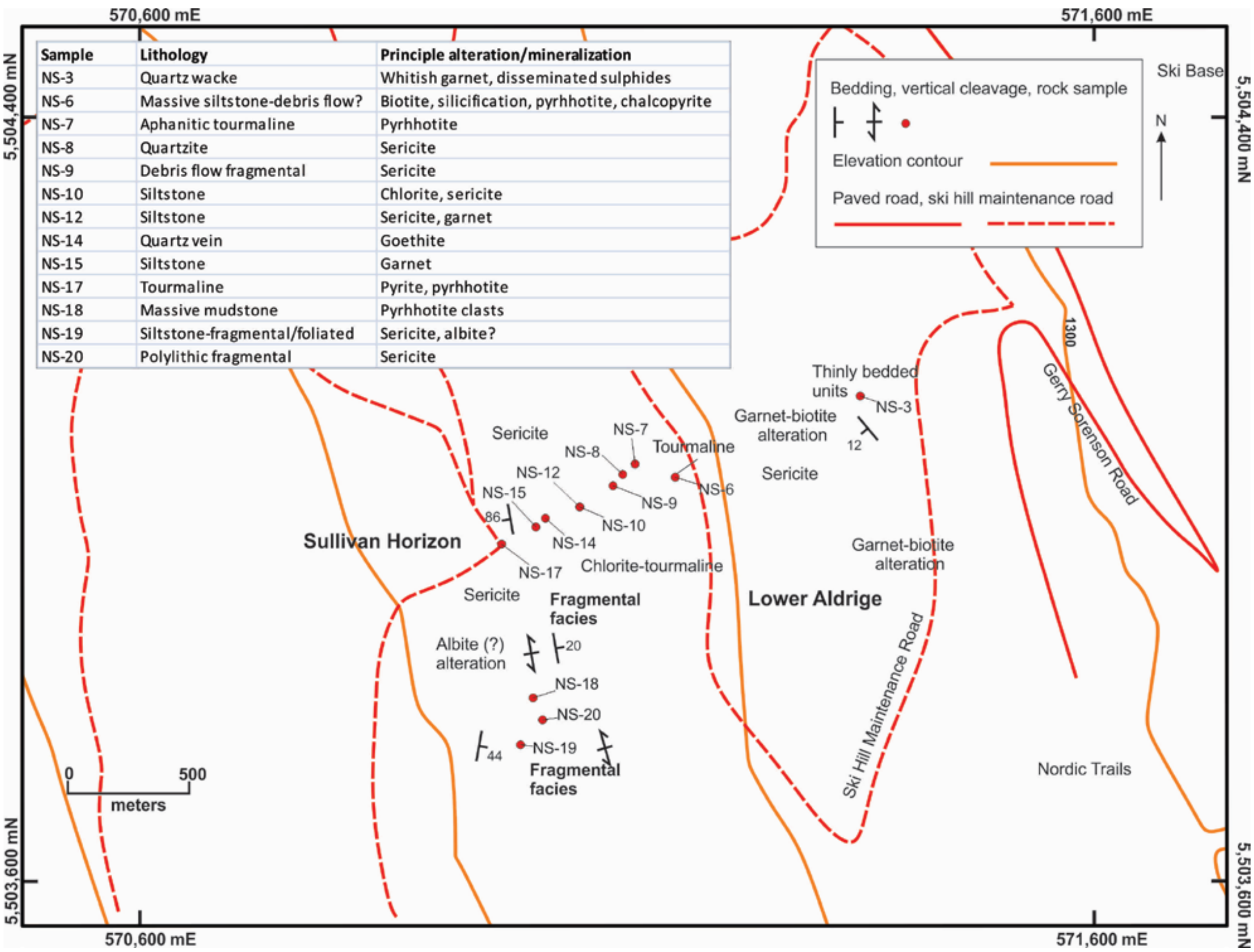

Sample	Lithology	Principle alteration/mineralization
NS-3	Quartz wacke	Whitish garnet, disseminated sulphides
NS-6	Massive siltstone-debris flow?	Biotite, silicification, pyrhhotite, chalcopyrite
NS-7	Aphanitic tourmaline	Pyrhhotite
NS-8	Quartzite	Sericite
NS-9	Debris flow fragmental	Sericite
NS-10	Siltstone	Chlorite, sericite
NS-12	Siltstone	Sericite, garnet
NS-14	Quartz vein	Goethite
NS-15	Siltstone	Garnet
NS-17	Tourmaline	Pyrite, pyrhhotite
NS-18	Massive mudstone	Pyrhhotite clasts
NS-19	Siltstone-fragmental/foliated	Sericite, albite?
NS-20	Polylithic fragmental	Sericite

***Figure 6.** Sample location map for North Star hill with alteration notes.*

Table 5. *Geochemical analyses from North Star (*30 g sample assayed with a 1DX 36 element ICP, *Bureau Veritas, Vancouver).*

Sample	Mo	Cu	Pb	Zn	Ag	Ni	Co	Mn	Fe	As	Au	Th	Sr	Cd	Sb	Bi	V	Ca
	PPM	PPM	PPM	PPM	PPM	PPM	PPM	PPM	%	PPM	PPB	PPM	PPM	PPM	PPM	PPM	PPM	%
NS-3	0.4	24.1	214.9	79	1.0	11.4	6.8	425	3.39	2.8	0.5	7.7	7	0.2	0.3	3.8	13	0.37
NS-6	1.6	62.0	938.3	384	3.4	13.5	7.4	554	5.23	3.5	15.6	10.8	4	1.1	1.6	15.6	23	0.16
NS-7	1.9	73.4	30.5	74	0.1	10.9	8.5	471	4.54	8.7	4.7	12.0	4	0.1	3.8	0.2	9	0.16
NS-8	1.7	52.5	103.8	155	0.2	5.6	2.6	252	3.52	88.3	1.5	10.7	3	0.3	1.7	0.3	9	0.10
NS-9	1.8	15.9	32.5	31	0.1	0.6	0.5	405	3.50	49.6	0.5	11.0	6	0.1	1.2	0.3	13	0.03
NS-10	1.0	8.2	42.3	55	0.1	0.6	0.7	313	2.85	33.9	0.5	11.5	4	0.1	0.4	0.7	9	0.03
NS-12	1.9	27.3	228.2	19	0.3	0.4	0.1	52	1.23	0.9	2.3	9.9	6	0.2	2.3	0.6	4	0.06
NS-14	0.7	25.1	245.4	445	1.4	1.9	1.3	185	4.04	18.3	64.8	5.6	2	0.4	4.0	23.1	2	0.01
NS-15	2.5	20.9	70.8	630	0.1	4.5	2.5	735	3.09	1.9	7.2	13.0	2	1.9	0.6	0.2	11	0.09
NS-17	1.7	55.8	218.5	13	0.2	3.9	2.2	251	1.71	47.5	5.9	6.5	2	0.1	2.8	1.2	3	0.13
NS-18	2.4	42.1	33.9	163	0.1	14.1	3.8	852	4.73	13.5	1.0	11.9	3	0.2	3.3	0.3	14	0.09
NS-19	1.0	5.9	204.8	14	0.3	0.1	0.1	179	0.53	3.8	0.5	4.3	6	0.1	1.6	0.1	2	0.01
NS-20	1.8	23.1	128.9	41	0.4	0.9	0.3	470	3.92	6.7	0.7	12.5	11	0.1	1.6	1.0	17	0.02
Sample	**P**	**La**	**Cr**	**Mg**	**Ba**	**Ti**	**B**	**Al**	**Na**	**K**	**W**	**Hg**	**Sc**	**Tl**	**S**	**Ga**	**Se**	**Te**
	%	PPM	PPM	%	PPM	%	PPM	%	%	%	PPM	PPM	PPM	PPM	%	PPM	PPM	PPM
NS-3	0.028	20	15	0.48	26	0.097	2	1.23	0.007	0.26	1.0	0.01	2.2	0.2	0.64	3	0.5	0.2
NS-6	0.044	28	21	0.82	49	0.153	1	1.94	0.003	1.30	4.8	0.01	2.6	2.2	1.65	6	0.5	0.2
NS-7	0.047	25	9	0.65	30	0.072	9	1.06	0.007	0.63	1.3	0.01	1.7	1.7	2.31	3	0.5	0.2
NS-8	0.042	21	9	0.50	32	0.082	2	1.01	0.005	0.71	1.7	0.01	1.4	1.9	0.89	3	0.5	0.2
NS-9	0.046	25	12	0.46	78	0.109	2	1.15	0.006	0.92	4.8	0.01	1.4	2.2	0.30	3	0.5	0.2
NS-10	0.043	22	10	0.53	47	0.038	1	1.42	0.006	0.46	3.0	0.01	1.7	0.7	0.05	4	0.5	0.2
NS-12	0.022	19	5	0.03	38	0.071	1	0.36	0.007	0.32	3.4	0.02	1.1	0.8	0.36	2	0.5	0.2
NS-14	0.017	22	2	0.02	26	0.001	2	0.23	0.008	0.22	1.0	0.05	0.9	0.2	0.07	1	0.5	0.2
NS-15	0.042	36	11	0.52	67	0.067	3	1.45	0.007	0.60	0.5	0.01	1.8	1.0	0.42	4	0.5	0.2
NS-17	0.039	5	3	0.03	25	0.077	33	0.28	0.008	0.18	0.3	0.01	1.0	0.2	0.66	1	0.5	0.2
NS-18	0.043	15	11	0.54	42	0.086	18	1.19	0.005	0.74	0.3	0.01	2.0	1.9	1.62	3	0.5	0.2
NS-19	0.016	10	2	0.03	59	0.018	1	0.31	0.005	0.26	0.1	0.04	0.6	0.3	0.05	1	0.5	0.2
NS-20	0.038	24	15	0.57	80	0.149	1	1.43	0.005	1.14	0.3	0.01	2.1	2.6	0.24	4	0.5	0.2

NS-3 (quartz-wacke), NS-6 (siltstone; biotite, silicification), NS-7 (siltstone; tourmaline), NS-8 (quartzite), NS-9 (fragmental; biotite), NS-10 (siltstone; chlorite), NS-12 (siltstone; sericite, garnet), NS-14 (quartz vein; goethite), NS-15 (siltstone; garnet), NS-17 (tourmalinite), NS-18 (fragmental), NS-19 (fragmental; albite, sericite), NS-20 (polylithic fragmental)

Pakk

Location, Access and Physiography

The Pakk prospect is located south of St. Mary Lake in the headwaters of Jack Creek (Jack Creek Basin), a tributary of Hellroaring Creek, at UTM 551,800mE and 5,489,500mN (Figure 2). Access to the area is provided by a steep diamond drill road located at the end of the Jack Creek Forest Service Road. The area covers a narrow talus-covered basin flanked by steep ridgelines predominantly above tree-line. Elevation within the immediate area of the Pakk ranges from 2100 to 2500 m. Outcrop exposure is limited to steep ridge lines and cliff faces with some minor exposures near the centre of the basin.

Geology

Middle Aldridge Formation sedimentary rocks and gabbroic sills outcrop extensively in the headwaters of Jack Creek (Brown et al., 2011c). Bedding attitudes are generally oriented north-south and dip moderately to steeply west. The Pakk area is located approximately 4 km north, and within the hanging wall, of the northeast-trending, northwest-dipping, St. Mary reverse fault which juxtaposes Aldridge Formation against younger stratigraphies. Stratigraphically the Jack Basin is in the middle portion of the Middle Aldridge as defined by the regional marker column (see Figure 2).

At the Pakk, a 150 m wide by 1.2 km long, east-west trending structural zone referred to as the Jack Pipe cuts Middle Aldridge Formation units (Figures 7A and 8). The vertical extent of the Pipe from the highest outcrop to drill hole intersections is in excess of 230 m. The Jack Pipe occurs in the footwall of the regional Sundown sill at the intersection of several faults and is delineated by a series of discordant fragmental dykes, a gabbroic dyke swarm, hydrothermal alteration, and base metal mineralization. The west end of the Jack Pipe is offset to the south about 300 m in a left-lateral sense by the northwest-trending Evans Fault. Prospecting east of the Pakk Fault indicates that the structure continues into the headwaters of Sinclair Creek (Kennedy, T., personal communication, 2015).

History

In 1999 three short diamond drill holes were completed to test the discordant fragmental units and dyke complex (Anderson and Klewchuk, 2000). Drill hole P99-1 intersected a continuous 12 m zone of fragmental rocks composed of altered sedimentary clasts in a gabbroic matrix underlain by a zone of discordant sedimentary fragmental rocks. Both fragmental units were mineralized with sphalerite, galena, chalcopyrite, arsenopyrite, and pyrrhotite. Drill hole P99-2 intersected a clast- to matrix-supported sedimentary fragmental unit, over a 3.6 m interval that was underlain by a 13.2 m wide albitized crackle breccia. Both fragmental and albitic breccias contained galena, sphalerite, arsenopyrite, and pyrrhotite. The third hole drilled during the program failed to intersect the fragmental complex due to faulting. In 2004, a 1768 m hole was collared north of the Jack Pipe, on the west side of the Pakk Fault, to test for Sullivan Horizon at the Lower Aldridge-Middle Aldridge contact (Anderson, 2006). The hole deviated to the northwest and intersected an anomalously thick package of disrupted and fragmental rocks at Sullivan-time. Drill hole P-00-15, which was collared 1500 m to the north, intersected a much thinner package of fragmental rocks at Sullivan-time indicating the Pakk area was an active structural block during deposition of the Sullivan (Anderson, 2006).

Description of Fragmental Units

Fragmental rocks at the Jack Pipe are best exposed immediately east of the northwest-trending Evans Fault where they form a series of east-west trending, steeply-dipping discordant bodies cutting shallow to moderately southwest-dipping sedimentary strata (see Figure 8).

Two distinct discordant fragmental types were identified in the Jack Pipe. The first type of fragmental rock is a clast- to matrix-supported discordant clastic dyke (Figure 7B). Clasts within the unit are angular, vary in size from mm to dm in diameter and are variably altered to tourmaline. Decimeter to cm scale channels are defined by angular sedimentary clasts, and glassy, broken sand-sized grains infill the larger discordant breccias. Individual breccias can exceed 10 m in width. Locally, sedimentary units are disrupted and incorporated into the breccias.

The second type of fragmental rock in the Jack Pipe cuts the tourmalinized breccia unit. It may represent a mafic magmatic breccia characterized by cm to dm albitic and chloritic fragments with diffuse edges incorporated within a fine-grained chlorite, actinolite, garnet, and zoisite(?) matrix.

The Jack Pipe structural zone hosts a series of gabbro-diorite dykes. These intrusions tend to be thin anastomizing strands with sharp contacts that coalesce into individual bodies over 10 m wide. The dykes have been metamorphosed to actinolite, chlorite, and zoisite and contain large reddish garnet porphyroblasts. All the observed fragmental units are spatially associated with gabbroic dykes, either occurring immediately along, or within a few meters of, a dyke contact.

On the west side of the Evans Fault the Jack Pipe system becomes discontinuous and 'horsetails' into the host sedimentary sequence. Irregular gabbro and lamprophyre dykes in this area occupy narrow east-west trending structural zones associated with minor soft-sediment deformation and later brittle deformation. A poorly exposed semi-conformable zone of disrupted beds and rip-up clasts showing albite and chlorite alteration occurs approximately 30 m below the footwall of the Sundown sill (Figure 7 C).

Mineralization and Alteration

At least four types of base metal mineralization were noted at the Pakk. Vein and disseminated sulphide mineralization, including galena, sphalerite, chalcopyrite, arsenopyrite, pyrrhotite, and pyrite, is associated with a metamorphosed alteration assemblage consisting of actinolite, albite, biotite, chlorite, garnet, iron carbonate, zoisite and quartz. This mineralization and alteration assemblage appears to be local to the Jack Pipe corridor, infilling fractures and replacing(?) some of the matrix within the fragmental units.

Coticule (spessartine metapelite) beds similar to those described from the Sullivan graben (Slack et al., 2000) occur in numerous, narrow (cm scale) horizons adjacent to the Jack Pipe. These horizons, which contain abundant biotite, tourmaline needles, disseminated garnet, disseminated arsenopyrite and rare disseminated sphalerite, can be traced 100's of meters laterally from the pipe.

Stratabound copper mineralization and associated biotite alteration (Figure 7 D) occur along two laterally extensive horizons (~1 m thick) in the footwall of the Sundown sill west of the Evans Fault below the semi-conformable disrupted zone described above (Figure 7 C). The two beds are separated by a few meters of more typical Middle Aldridge units. The mineralized beds contain visually abundant disseminated chalcopyrite with rare native copper. In the field these copper-bearing horizons form white- to rusty-weathering, finely-banded outcrops with mm-scale rounded nodules composed of biotite with sulphide cores. The two horizons have been traced over 1.5 km to the southwest (Kennedy, T., personal communication, 2015).

Lastly, galena, sphalerite, and pyrite within late stage quartz veins, shear zones, and fractures associated with albitic and chloritic breccias and silicification occur throughout the Jack Creek basin.

Structure

Bedding attitudes in the Jack Creek basin dominantly strike north-northwest and dip moderately to the west. Syn-sedimentary deformation appears to be restricted to the immediate area of the Jack Pipe. An early east-west structural trend defined by the Jack Pipe is offset by the northwest-trending Evans Fault. The north-northeast trending Pakk Fault shows late movement but is interpreted to be a growth structure based on changes within the sedimentary facies of the Lower Aldridge Formation (Anderson, D., personal communication, 2015). Local drag folding occurs along numerous late stage brittle faults within the larger Jack Creek basin. Numerous steeply dipping northerly-trending faults are visible within the basin walls north of the Jack Pipe.

Sampling

Three samples were selected for analysis from the Jack Pipe (Table 6 and Figure8). The samples were taken from discordant tourmaline clast breccias with visible base metals associated with actinolite, albite, biotite, chlorite, garnet, iron carbonate, zoisite and quartz. This alteration/mineralization suite is spatially associated with the Pipe and was therefore considered to be genetically related to the fragmental process. Selective sampling of the tourmaline breccias showed elevated values for base metals up to; Pb 5716 ppm, Zn 6912 ppm, and Cu 210 ppm (sample PAKK-1). Additionally the samples showed elevated values for silver, arsenic, bismuth, manganese, nickel, vanadium, chromium, and tungsten.

Interpretation

The Jack Pipe is interpreted to be a discordant mud-volcano feeder dyke system occurring at the intersection of north-south and northwest-trending structures. Due to erosion, the root of the system has been exposed without evidence of an intact hanging wall mud-volcano that may have been developed above the feeder. Two distinct styles of discordant fragmental units (earlier tourmaline clast breccias, and later magmatic breccias) occupy the structural corridor. Base metal mineralization is associated with a metamorphosed alteration suite similar to the composition of the later magmatic breccias and gabbro dykes and is therefore considered to be related to this event.

Figure 7. *Field photos of the Pakk Prospect. A) Looking east along the extension of the Jack Pipe towards the Sinclair-Jack Creek ridge. B) Tourmalinized discordant fragmental in the Jack Pipe. C) Albitized and chlorite rich semi-conformable rip-up fragmental below the Pakk Cu horizon. D) Pakk Cu horizon.*

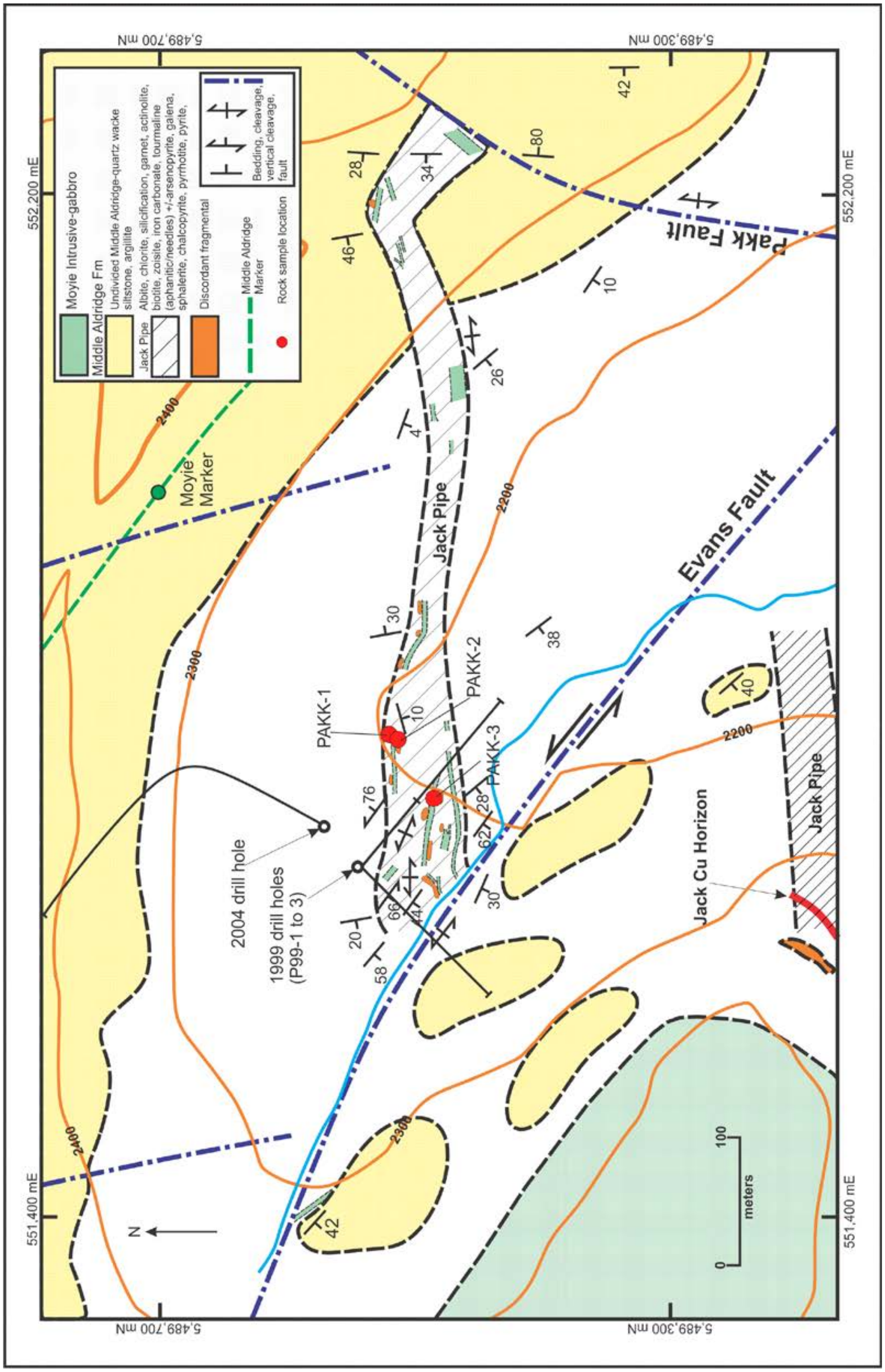

__Figure 8.__ Geology of the Pakk area.

Table 6. *Geochemical analyses from the Pakk, Ryder, and Rise areas.*

	Mo	Cu	Pb	Zn	Ag	Ni	Co	Mn	Fe	As	Au	Th	Sr	Cd	Sb	Bi	V	Ca
Sample	**PPM**	**PPM**	**PPM**	**PPM**	**PPM**	**PPM**	**PPM**	**PPM**	**%**	**PPM**	**PPB**	**PPM**	**PPM**	**PPM**	**PPM**	**PPM**	**PPM**	**%**
PAKK 1	0.5	210.6	5716.2	6912	3.4	53.9	18.9	1505	9.46	20.4	0.5	4.9	11	39.5	0.4	8.3	181	0.44
PAKK 2	0.3	8.4	82.3	246	0.1	30.6	8.8	1425	3.99	172.9	0.5	1.3	31	1.0	0.2	0.2	105	1.01
PAKK 4	0.5	46.9	10.3	98	0.1	13.5	4.8	941	2.66	10.3	0.5	11.4	14	0.3	0.1	0.3	20	0.42
RY-2	0.3	18.8	43.5	33	0.1	4.5	3.2	134	1.22	2.4	0.5	10.5	10	0.2	0.2	0.3	9	0.07
RY-3	0.9	13.8	7.0	23	0.1	2.9	1.7	74	1.83	0.5	0.5	15.8	29	0.1	0.2	0.4	11	0.02
RY-5	0.4	9.3	17.5	39	0.1	3.4	2.6	298	3.08	0.5	0.5	14.8	10	0.1	0.2	0.4	17	0.07
RY-10	0.6	11.0	16.9	33	0.1	4.9	3.1	196	2.41	0.6	0.5	13.0	6	0.1	0.1	0.5	13	0.04
RY-18	0.9	45.8	67.2	429	0.2	30.9	12.0	247	2.31	0.5	0.5	10.9	7	2.4	0.4	0.5	20	0.17
RY-20	0.5	28.2	14.2	54	0.1	16.4	6.9	246	1.30	2.3	0.5	9.7	39	0.3	0.2	0.2	19	0.43
RY-22	0.1	0.9	30.4	92	0.1	7.8	3.6	273	1.12	1.3	0.5	15.6	57	0.2	0.2	0.1	12	0.43
RISE 1	1.1	9.9	12.8	13	0.2	13.4	29.3	79	1.25	5825.4	69.0	12.0	10	0.1	2.6	16.6	30	0.03
RISE 2	2.7	7.8	4.7	4	0.1	5.3	0.9	25	0.45	27.1	15.9	11.6	4	0.1	0.7	11.2	3	0.06
RISE 3	0.6	8.4	6.4	7	0.1	1.8	0.3	27	0.79	7.4	0.5	7.3	8	0.1	0.2	4.0	5	0.01
F3	0.3	25.6	14.9	67	0.1	21.3	12.9	314	3.13	47.4	1.0	15.3	6	0.1	0.3	0.2	19	0.03
F6	1.3	16.0	20.1	54	0.1	5.9	2.7	189	3.00	30.3	1.1	15.5	15	0.1	0.3	0.4	20	0.02
F9	0.2	5.9	18.3	9	0.1	5.3	1.0	38	0.60	4.6	1.4	9.4	3	0.1	0.1	0.2	3	0.01
F13	0.3	3.7	9.0	30	0.1	13.8	3.3	97	1.18	7.6	0.5	18.4	3	0.1	0.2	0.2	9	0.06
Sample	**P**	**La**	**Cr**	**Mg**	**Ba**	**Ti**	**B**	**Al**	**Na**	**K**	**W**	**Hg**	**Sc**	**Tl**	**S**	**Ga**	**Se**	**Te**
	%	**PPM**	**PPM**	**%**	**PPM**	**%**	**PPM**	**%**	**%**	**%**	**PPM**	**PPM**	**PPM**	**PPM**	**%**	**PPM**	**PPM**	**PPM**
PAKK 1	0.038	17	141	1.78	102	0.348	2	4.11	0.029	2.13	0.4	0.01	17.1	1.3	1.81	11	0.5	0.2
PAKK 2	0.035	4	97	1.47	71	0.227	1	2.46	0.027	0.77	0.4	0.01	6.7	0.8	0.05	5	0.5	0.2
PAKK 4	0.022	23	18	0.50	16	0.107	12	1.36	0.026	0.13	0.6	0.01	2.9	0.1	0.15	4	0.5	0.2
RY-2	0.017	34	11	0.14	59	0.057	1	0.46	0.056	0.19	0.1	0.01	1.4	0.1	0.18	2	0.5	0.2
RY-3	0.037	27	10	0.31	141	0.074	1	1.16	0.020	0.75	0.1	0.01	1.3	0.5	0.18	3	0.6	0.2
RY-5	0.049	33	15	0.62	173	0.143	1	1.52	0.018	1.12	0.1	0.01	1.7	0.8	0.17	4	0.5	0.2
RY-10	0.030	20	12	0.42	120	0.095	1	1.26	0.025	0.71	0.1	0.01	1.5	0.5	0.05	3	0.5	0.2
RY-18	0.068	21	16	0.67	108	0.098	1	1.34	0.023	0.85	0.1	0.01	1.7	1.0	0.65	4	0.5	0.2
RY-20	0.017	17	18	0.34	37	0.097	1	1.48	0.052	0.13	0.1	0.01	3.2	0.2	0.22	4	0.6	0.2
RY-22	0.018	21	16	1.76	56	0.149	1	1.86	0.015	0.41	0.1	0.01	1.4	0.2	0.05	5	0.5	0.2
RISE 1	0.031	36	15	0.71	50	0.037	5	1.04	0.015	0.75	0.1	0.01	3.8	0.7	0.26	3	3.8	1.9
RISE 2	0.040	47	3	0.07	34	0.004	11	0.42	0.011	0.26	0.1	0.01	1.1	0.2	0.05	1	1.0	0.8
RISE 3	0.021	23	5	0.30	29	0.012	1	0.58	0.013	0.45	0.1	0.01	1.3	0.3	0.08	2	8.3	0.2
F3	0.035	48	20	0.51	52	0.016	1	1.36	0.013	0.20	0.1	0.01	2.5	0.2	0.05	5	0.5	0.2
F6	0.037	37	18	0.75	104	0.126	1	1.51	0.024	1.05	0.1	0.01	2.5	0.8	0.15	4	0.5	0.2
F9	0.007	24	5	0.04	27	0.014	2	0.21	0.026	0.09	0.1	0.01	0.9	0.1	0.05	1	0.5	0.2
F13	0.033	36	9	0.27	82	0.039	1	0.84	0.017	0.41	0.1	0.01	1.7	0.2	0.05	3	0.5	0.2

PAKK 1 (discordant fragmental; actinolite, garnet, albite, chlorite, galena, sphalerite, chalcopyrite), PAKK 2 (discordant fragmental; tourmaline, albite, chlorite, sphalerite), PAKK 4 (discordant fragmental, tourmaline, albite, chlorite), RY-2, 3, 5 (fragmental mound; biotite, sericite), RY-10 (fragmental mound; sericite), RY-18 (varved siltstone; galena, sphalerite), RY-20 (debris flow; albite, chlorite, garnet), RY-22 (exhalite; tremolite, calcite), RISE 1 (Discordant fragmental; arsenopyrite, biotite), RISE 2 (varved siltstone; tourmaline), RISE 3 (discordant fragmental; albite, sericite), F3 (discordant fragmental; chlorite, sericite), F6 (fragmental; sericite), F9 (massive quartzite; biotite, chlorite), F13 (discordant fragmental; biotite)

Ryder

Location, Access, and Physiography

The Ryder area is located east of Ryder Creek in the Moyie River drainage centered at UTM 567,200mE and 5,470,800mN (Figure 1). Access is provided by the Lumberton Forest Service Road which branches off of Highway 95, 12 km south of Cranbrook, BC. The area is located between 1700 and 1900 m elevation. Topography is moderate and dominantly tree-covered with a limited outcrop.

Geology

Stratigraphically the Ryder fragmental unit is located between the Hiawatha and Sundown sills near the middle of the Middle Aldridge Formation (Brown et al., 2011a) based on the regional marker column (Figure c). It is located north of the northeast-trending Moyie River normal fault along the east flank of a shallowly north-plunging open anticline.

Description of Fragmental Units

During the program fragmental rocks at Ryder were subdivided into basal, middle, and upper divisions which have a maximum aggregate thickness of approximately 105 m (Figure9). The fragmental complex is exposed along a north-northeast trend for over 600 m and has an elliptical shape. It remains open to the north and is inferred to be controlled by a northwest-trending structure along the southwest margin of its basal unit. The upper two units overlap this inferred structure and finger out into Middle Aldridge units to the southwest. Debris flow fragmental units are exposed down slope, and down section of the basal division.

The basal unit of the fragmental complex is approximately 50 m thick. It forms a bluff of massive sericitic quartz arenite to wacke with matrix-supported, fine-grained, mm to cm scale quartzite clasts, and lenses of polylithic (argillite, siltstone, quartzite) clast-dominated (mm to dm scale) fragmental rock. Clasts within the fragmental unit are angular to sub-rounded and typically show a preferred alignment, which, in some cases, defines an approximate bedding orientation. The basal unit abuts more typical Middle Aldridge turbidites along an inferred northwest-trending structure. Intermittent thin zones of clast-rich fragmental rocks and local massive, poorly-bedded debris flow units finger out into the section to the southwest.

Capping the basal unit is an approximately 40 m thick interval of locally disrupted laminated biotitic to sericitic, thin to medium-bedded, quartz wacke and argillaceous siltstone (Figure 10 A). Slump structures, massive units, soft-sediment deformation, rip-up clasts and lenses of clast-dominated fragmental are characteristic of this unit. Interbedded within the unit is an unidentified Middle Aldridge marker bed that was traced discontinuously across the hillside for over 650 m. Locally, the marker bed is incorporated into the slumped and disrupted zones. The unit shows a distinctive hematitic to goethitic mottling and sericitic bleaching on weathered surfaces. It is differentially weathered in places displaying a rounded to pitted character.

The highest unit within the fragmental complex is a poorly bedded, bulbous weathering, dark grey to black siltstone unit that is draped over the middle member. This unit is approximately 15 m thick and is composed of disrupted beds and rip-up clasts containing mm to cm scale ragged argillaceous clasts in a dark grey silty matrix.

Structure

The Ryder fragmental units are hosted in shallow north to northeast-dipping strata along the east flank of a broad north-plunging anticline. Northwest-trending syn-sedimentary structures have been inferred along the southwest boundary of the basal member of the fragmental complex. These structures host late stage quartz-magnetite-gold-bearing crackle breccias. A north-trending phyllitic shear zone was mapped west of the main fragmental units.

Mineralization and Alteration

The sulphide mineralization of the fragmental package is best developed within the middle unit, where disseminated pyrrhotite and pyrite occur in thin-bedded laminated greywacke and argillaceous siltstone. Minor galena and sphalerite are present in sericitic veinlets and weakly disseminated in strongly sericitized and albitized (?) quartz wacke and pyrrhotite-rich laminated argillaceous siltstone.

Sericite alteration occurs as fine disseminations, in fractures, as patches in the basal unit and more pervasively (Figure 10B) in the middle division where it is mostly present in silicified lenses that contain albite (?), pink garnet and actinolite. Subcrop bearing fibrous actinolite with calcite was found near the contact of the basal unit and overlying middle member. The subcrop shows faint laminations interpreted as relict bedding. Liesegang alteration, bleaching, and manganese oxides related to late, visible gold-bearing quartz magnetite veins and breccias, crosscut the middle unit and adjacent turbidite sequences (Figure 10). These veins are localized along northwest trends parallel to the contact of the fragmental unit.

Sampling

Seven samples were collected from the fragmental area (Table 6 and Figure 9). One sample contained weakly disseminated sphalerite (RY-18, 429 ppm Zn) while the results for the remaining rock samples were consistent with background values for fragmental units based on Cominco’s work (see Table 4).

Interpretation

The Ryder area covers three distinct fragmental facies that are interpreted to represent a mud volcano complex that extruded onto the seafloor filling a local depression and forming a mound. The entire fragmental complex has an elliptical shape and trends northeast 600 m and is at least 350 m wide.

The basal unit of the fragmental complex is approximately 50 m thick and is interpreted to be a depression-fill, vent proximal body. The basal unit thickens east of a series of northwest-trending structures that are interpreted as growth faults. These structures are characterized in the field by rapid changes in the stratigraphy from turbiditic sediments to the basal fragmental unit, tightly spaced steep dipping cleavages, localized slump folding, alteration (including late quartz-magnetite-gold veins), and topographic lows. Intermittent thin zones of clast-rich fragmental rocks and local massive, poorly-bedded units within the turbidites southwest of the main fragmental units suggest that the basal unit was a mound from which debris flow deposits interbedded with the surrounding sediments. Debris flow fragmental rocks are also exposed down slope, and down section, of the basal division to the south, suggesting that mud volcano development was occurring into the footwall of the Ryder fragmental complex.

The middle unit contains a sequence of debris flow deposits, likely derived from slope collapse, with intermittent sediment extrusion suggested by clast-rich fragmental rocks. A Middle Aldridge formation marker bed was mapped within this unit. Locally, the marker bed has been incorporated into the slumped and disrupted zones, indicating that the inferred control structures had relatively little offset during sedimentation.

The uppermost unit of the fragmental complex is composed of massive, bulbous-weathering, to crudely-bedded, fragmented dark argillaceous siltstone that may mark the waning of the mud volcano eruption.

Sericitic alteration and Liesegang oxidation are the most common expressions of alteration associated with the Ryder fragmental units. The Liesegang alteration is related to late stage, presumably Mesozoic, quartz-magnetite-gold veins that occupy the inferred northwest-trending growth structures. The middle unit of the fragmental complex is much more sulphidic and contains patches of sericite-albite(?)-garnet-actinolite alteration and zones of differentially weathered and pitted rock. Subcrop (described above) of massive to faintly-bedded actinolite and calcite discovered near the base of the middle unit may represent the metamorphosed product of an originally vented carbonate unit.

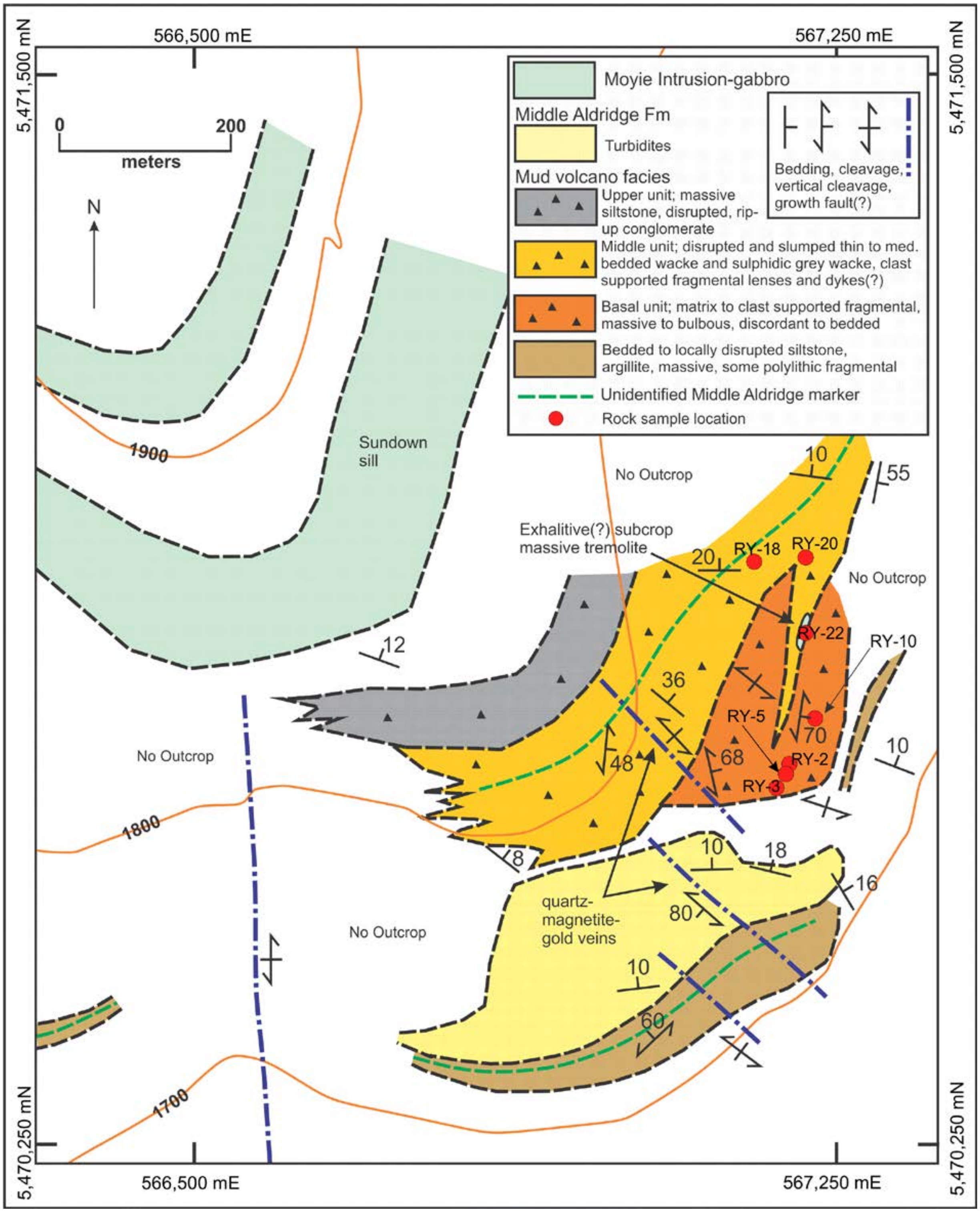

__Figure 9.__ Geology of the Ryder fragmental complex.

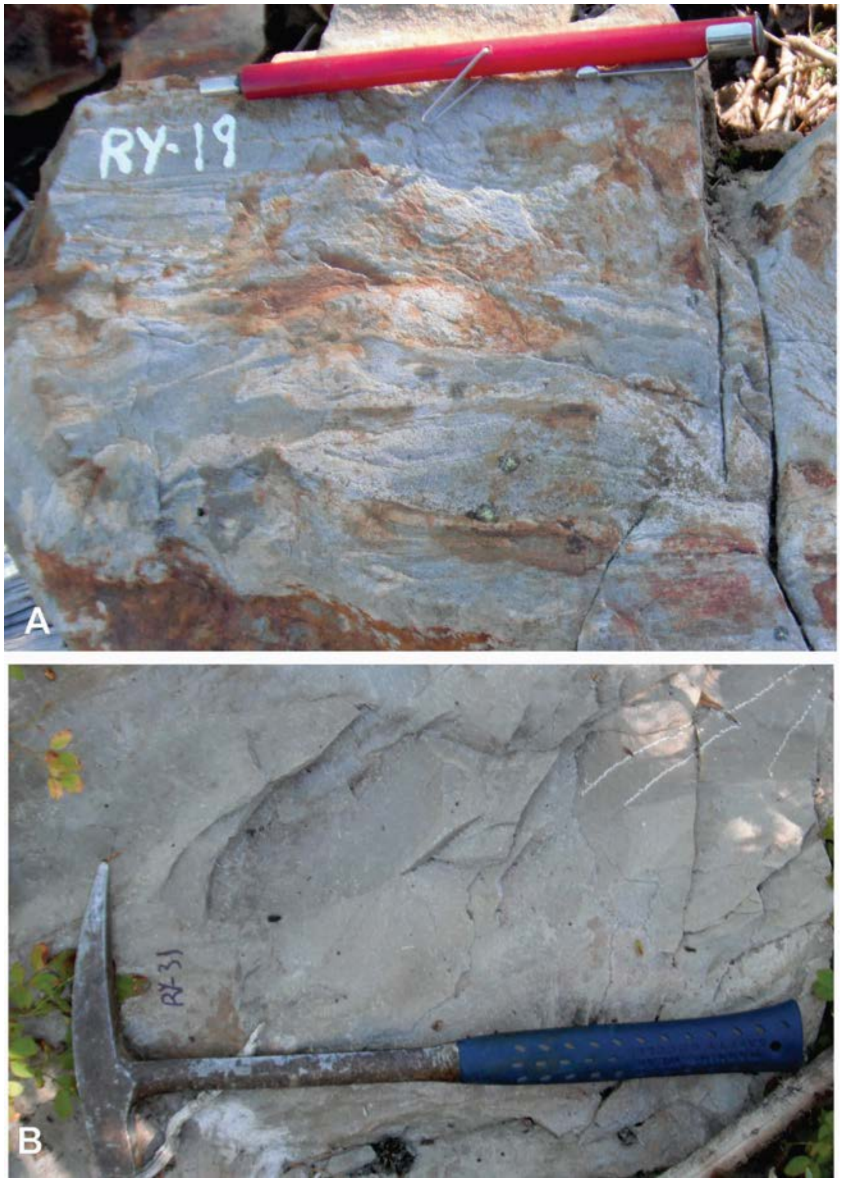

Figure 10. *Field photos from the Ryder area. A) Sericitic siltstone showing disrupted and convoluted bedding within the middle member of the Ryder fragmental unit. B) Pervasively sericitized fragmented siltstoneRise*

Rise

Location, Access, and Physiography

The Rise, North Farrell, and South Farrell fragmental units are exposed within a 1 x 1 km area south of Moyie Lake centered at UTM 584,700mE and 5,455,90mN (Figure 1). The area is accessed from the Sunrise Creek Forest Service Road which branches off of Highway 3, 3.5 km south of the village of Moyie. Topography within the study area is hilly and ranges from 1000 to 1200 m. Forest cover and overgrown logging cut-blocks cover the area. Outcrop is poor along the lower elevations and increases upslope and along logging roads.

Geology

The area is located along the eastern flank of the Moyie Anticline within the footwall of the Moyie Fault (Brown et al., 2011a). Regional bedding attitudes near the study area strike north-northwest and dip shallowly to the east. A series of north-trending faults cut through the area including the Ore Shoot Fault (Figure 11), a regional growth structure inferred in part by a linear trend of fragmental units that occur from near the international border to north of Moyie Lake (Pighin, D., personal communication 2015). Fragmental units in the Rise area are within the upper portion of the Middle Aldridge occurring near the R and Shaft marker horizons (Figure 3).

History

Exploration efforts at the Rise fragmental unit include a four-hole 2000 m drill program that was conducted in 1995 (Walker, 1996). All four holes were collared near the R marker horizon and drilled along an east-west section to test the fragmental unit for base-metal mineralization (Pighin, personal communication, 2015). One hole was drilled across the Rise fragmental showing it to be a steeply west dipping discordant zone (R95-1). The other holes drilled along the section line (R95-2,3,4) intersected three stacked fragmental beds (debris flows?) over a 750 m stratigraphic interval containing, tourmaline and garnet alteration, and disseminated and vein galena, sphalerite, and tetrahedrite.

Description of Fragmental Units

The Rise fragmental is exposed along a 100 m long and 30 m wide northwest trend. Outcrop is massive to locally fragmented siltstone to quartz-wacke with intense albite and sericite alteration. Massive fragmental rocks contain rare dark grey, elongate to deformed ragged fragments. Additional textures within the unit are difficult to identify in the field due to pervasive alteration and phyllitic cleavage. The fragmental unit is discordant to a lithologically distinct package of black and white/greyish thin-bedded, varved siltstones and quartzites that were mapped as the Rise mudstone during the program (Figure 11).

Fragmental rocks at North Farrell are crudely bedded and form a rounded mound-like structure approximately 100 x 100 m. Texturally the fragmental rocks are composed of sub-rounded clasts of argillite, siltstone, and quartz-wacke that range from mm to dm scale. Clasts are both matrix (quartz wacke) and clast-supported. A northeast-striking steeply-dipping discordant zone of fragmental rocks underlies the mound structure near its southwest contact (Figure 12). Bedded quartz wacke units which underlie the mound tilt abruptly into this discordant zone. Disrupted to massive sedimentary rocks overlie the unit, forming a broad domal feature. East of

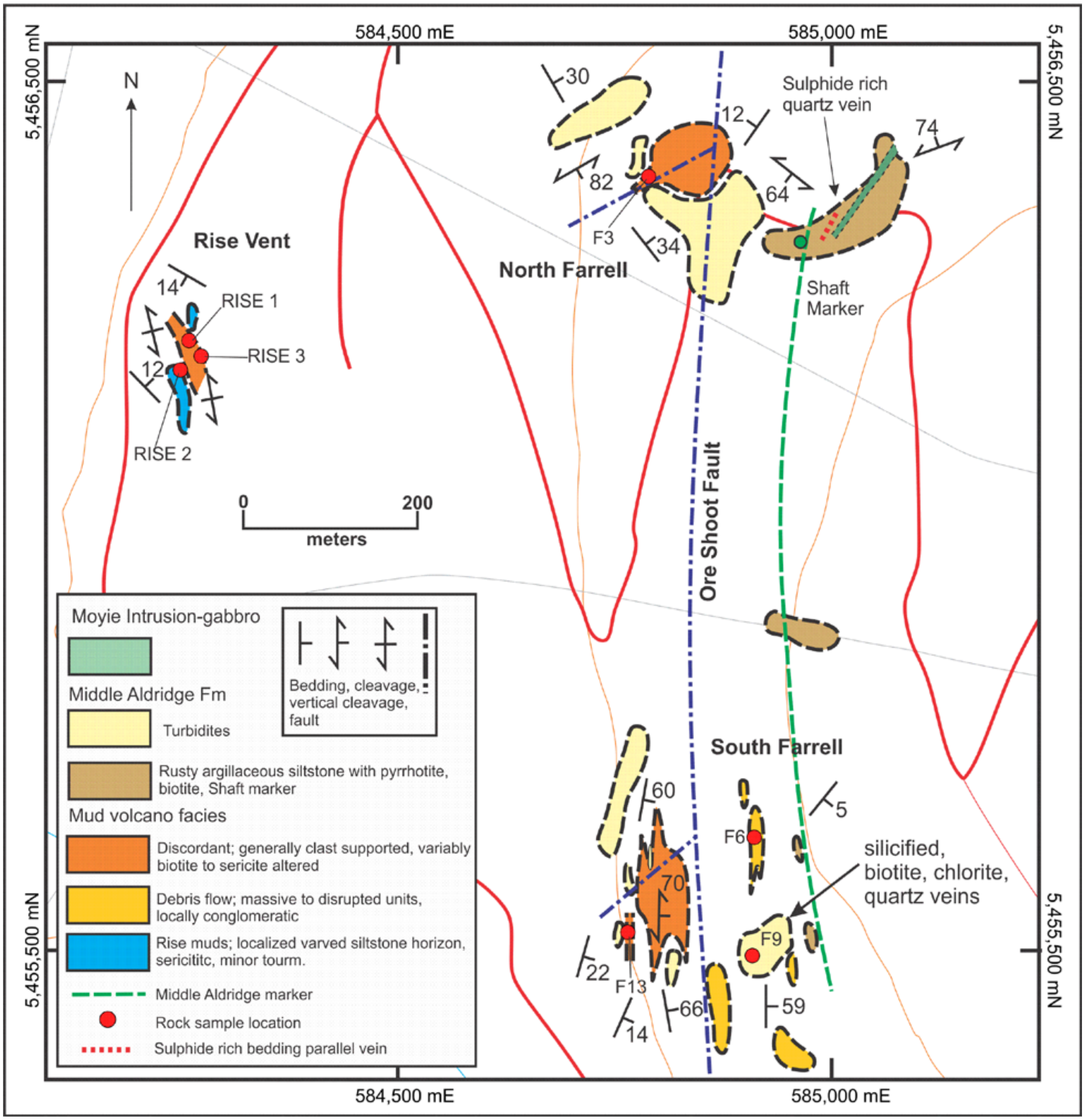

***Figure 11**. Geology of the Rise Vent area.*

Figure 12. *Photo showing the contact relationship of the North Farrell fragmental unit.*

the mound is a thick interval of pyrrhotite-rich, variably calcareous, laminated siltstone that hosts the Shaft marker horizon. A steeply-dipping northeast trending gabbro dyke and narrow zone of discordant mud-rich breccias cut the Shaft marker east of the main fragmental unit.

The South Farrell fragmental unit is located 850 m to the south at the same stratigraphic level where a series of steeply-dipping fragmental deposits tilt towards a north-south trending foliated zone. The fragmental unit is crudely elliptical and measures approximately 200 m x 75 m. It is enclosed to the north and south by more regular shallow dipping Middle Aldridge strata. Narrow biotite-rich clastic fragmental dykes are exposed in the stratigraphic footwall of the unit. It is overlain by massive sericitized and silicified quartz wacke and biotite-rich, massive, dark siltstone units.

Structure

Bedding attitudes proximal to all the fragmental units vary from the regional structural trends. At the Rise, flanking bedded units dip towards massive fragmental rocks forming a northwest-trending synclinal feature. At the North Farrell fragmental overlying strata form an anticline while underlying beds tilt into the base of the mound (Figure 12). At the South Farrell bedded rocks progressively tilt into the fragmental units forming a synclinal feature.

At the Rise fragmental unit an intensely developed cleavage (350º/90º) has overprinted the massive fragmental rocks locally imparting a phyllitic sheen. A similar phyllitic cleavage has overprinted fragmental rocks at South Farrell.

Both the North and South Farrell fragmental units occur at the intersection of the Ore Shoot Fault and northeast-trending structures.

Mineralization and Alteration

No base metal mineralization was observed at the three fragmental units. Minor stringers of arsenopyrite occur in biotite-rich lenses within highly albitized zones at the Rise. At North Farrel hornfelsed mudstone in the Shaft marker horizon adjacent to a northeast-trending gabbro dyke hosts a 20 cm wide bedding parallel quartz lens with massive pyrite and chlorite underlain by a mudstone breccia.

Intense sericite, biotite, and albite alteration has developed within the core of the Rise fragmental unit. The flanking Rise mudstone is intensely to pervasively sericite and biotite altered and locally replaced with tourmaline. Alteration at the North Farrell is restricted to a weak sericite and chlorite alteration zone within the underlying discordant fragmental unit.

At South Farrell biotite-rich, discordant clastic dykes and patchy tourmaline alteration underlie the main fragmental unit. Biotite alteration is also developed in overlying massive, disrupted to locally conglomeratic siltstone units that overlie the main fragmental unit. Sericite and albite alteration as well as goethite/hematite mottling is intensely developed within a massive quartz wacke unit that overlies the main fragmental unit to the southeast.

Sampling

Seven grab samples from altered fragmental rocks show no significantly elevated values for base metals (Table 6 and Figure 11). However one sample (Rise 1) of highly albitized and sericitized fragmental showed elevated values for arsenic, gold, antimony, and bismuth.

Interpretation

The Rise, North Farrell, and South Farrell fragmental units occur within a relatively small area at or near the same stratigraphic interval. They are interpreted to reflect a larger mud-volcano/hydrothermal vent field that was active during deposition of the upper part of the Middle Aldridge Formation.

The Rise fragmental unit is interpreted to represent the conduit zone of a long-lived hydrothermal vent system. The Rise mudstones are a unique lithology restricted to the immediate area flanking massive fragmental rocks at the Rise. Because the Rise mudstone is cut by the fragmental rocks it appears the system continued into the eroded hangingwall stratigraphy. Drilling conducted in 1995 across the Rise indicates that mud volcanism and hydrothermal alteration with associated base metal mineralization occurred well into the footwall of the surface showing (Walker, 1996).

The North Farrell fragmental unit is interpreted to be a vent-proximal mound underlain by a discordant northeast-trending feeder dyke (Figure 12). The South Farrell fragmental unit is interpreted to be a discordant pipe fragmental formed from repeated sediment extrusion and collapse into a central vent. The overlying debris flow deposits are interpreted to represent the waning of the mud-volcano and vent system.

SBA

Location, Access, and Physiography

SBA is centered at UTM 584,800mE and 5,451,500mN, approximately 7 km south of the village of Moyie (Figure 1). Access to the site is provided by taking the Sunrise Creek Forest Service Road located 3.5 km south of Moyie on Highway 3 and continuing on to the Sundown Forest Service Road after 3 km. The site is situated on the divide between Sundown and Sunrise Creeks between 1300 and 1500 m elevation. The area covers forested hilly to plateau-like topography that has recently been partly logged. Outcrop exposure is moderate at approximately 20%.

Geology

The geology of the Sundown Creek area has been compiled onto GSC Open File 6304 (Brown and MacLeod, 2011b). The area is located 4 km south of the Rise study area within the same structural block and shares many of the same features. The north-south trending Ore Shoot Fault, which cuts the Rise area, also cuts through the SBA area (Pighin, D., personal communication, 2015). Fragmental units at SBA are within the upper portion of the Middle Aldridge occurring near the R and Shaft marker horizons in the immediate hanging wall of the regional Meadowbrook sill and bracket the R sill (Figs. 3 and 13), the same stratigraphic position as the Rise and North and South Farrell fragmental units (Figs. 3 and. 11).

History

In 2011 prospector Craig Kennedy discovered an outcropping of polylithic clast-rich fragmental exposed by recent logging activity, and the following year he identified a number of galena-rich massive sulphide float boulders near the centre of the current SBA property (Figure 14). Mapping and rock and soil geochemistry conducted on the property in 2013 identified a large fragmental complex and alteration system (Kennedy, 2013).

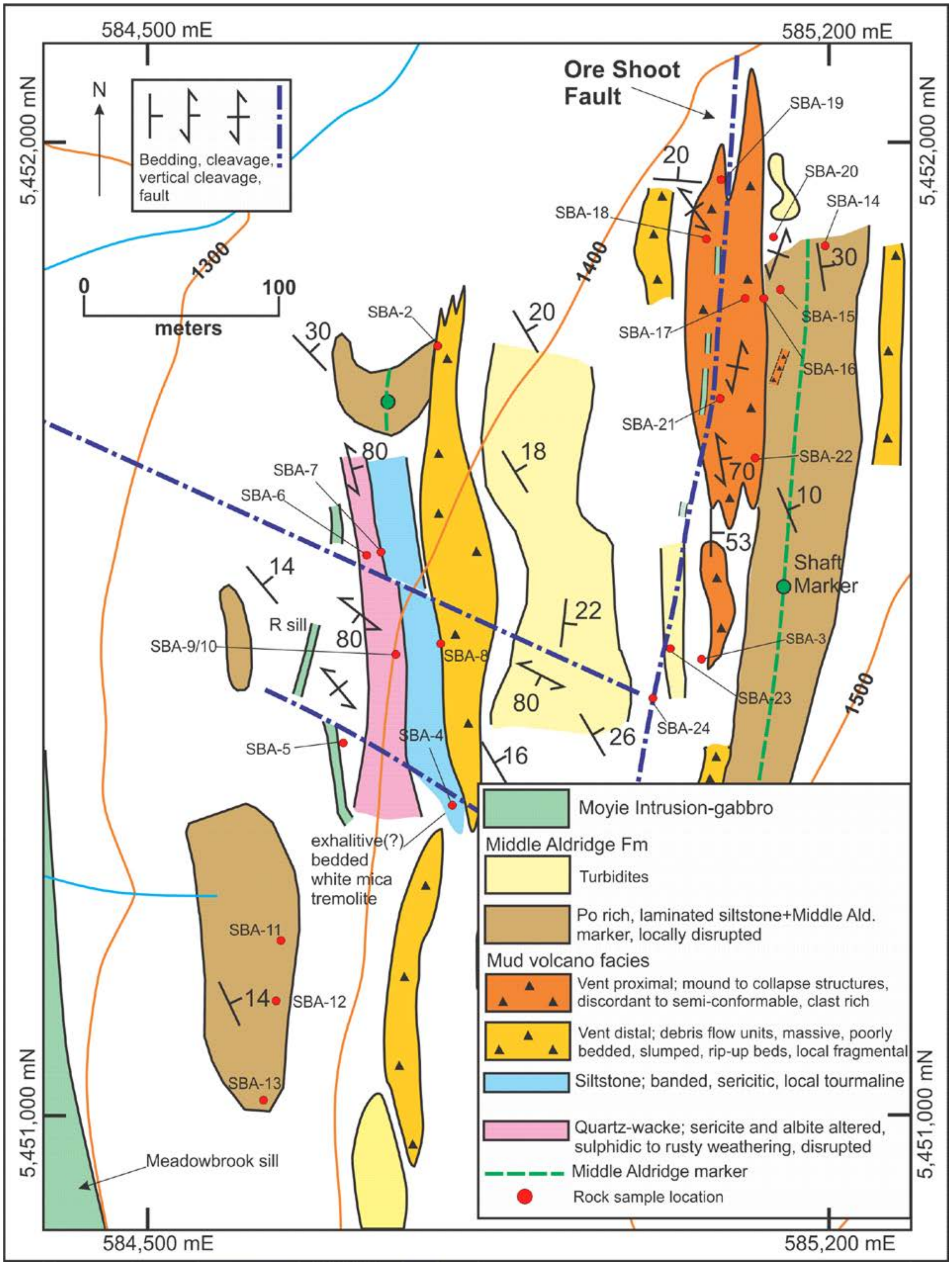

***Figure 13.** Geology of the SBA fragmental complex.*

Figure 14. *Massive sulphide (galena/sphalerite) float boulder with associated chlorite and garnet (SBA).*

Description of Fragmental Units

Fragmental units at SBA occur over a north-south oriented 1200 x 700 m area. The most extensive fragmental facies exposed in the area is an elongated elliptical mound-like structure that outcrops over 600 m with a maximum thickness of 35 m (Figure 13). Textures in the unit are well preserved and show both clast- and matrix-dominated phases. Clasts are polylithic (argillite, siltstone, quartzite), mm to dm scale, angular to sub-rounded and show a preferred orientation sub-parallel to local bedding attitudes (Fig 15 A). At the northern extension of the fragmental unit, underlying quartz wacke beds have been broken and tilted into a series of discordant fragmental 'tongues'. To the south, the mound structure appears to thin and finger out into a debris flow unit.

The mound structure is overlain by a 25 m thick sequence of pyrrhotite-rich argillaceous siltstone that hosts the Shaft marker. Within the marker-bearing siltstone is a series of north-south trending mud breccias and clastic dykes. One clastic dyke cutting the Shaft horizon has angular albitized(?) fragments showing a preferred alignment in a black silty matrix with minor galena (Figure 15 B). Overlying this horizon is another interval of debris flow fragmental rocks.

Underlying the mound deposit is a thick sequence of variably sulphidic and calcareous debris flow-type fragmental rocks that occurs near the R marker horizon (Figure 13). This unit is roughly 900 m long and 25 m thick. It is characterized by irregular bedding, massive units, slumping, and localized clast-rich fragmental rocks similar to the overlying mound deposit. This unit tapers into a massive siltstone to the north.

Below the debris flow units described above is a 380 m long, 25 m thick sequence of highly altered sericite- and biotite-rich, thinly bedded, varved siltstone and quartz wacke similar in appearance to the Rise mudstone (see Rise section above). Immediately underlying this unit is a sequence of irregularly bedded quartz wacke to arenite which overlie the R sill.

Structure

Bedding at the SBA typically strikes northwest with shallow to steep northeast dip towards the inferred Ore Shoot Fault. Localized deflections in bedding trends have been demonstrated to delineate northwest faults that show minor offset on the R sill.

The Ore Shoot Fault occupies the central and thickest portion of the mound structure described above. It is delineated by steep dips and an intermittently outcropping gabbro dyke as well as tightly-spaced vertical cleavage and alteration.

Mineralization and Alteration

Within the mound unit patchy sericite, chlorite, and biotite alteration is associated with increased concentrations of pyrrhotite and rare sphalerite. A series of thin sphalerite-, pyrite-, sericite-, and chlorite-rich northeast-striking (030˚) vertical veinlets cut the mound deposit adjacent to the Ore Shoot Fault. Chlorite is also associated with pyrrhotite and galena veinlets in the debris flow units underlying the mound structure in the vicinity of a northwest-trending fault. Massive sulphide boulders found in the vicinity of the fragmental occurrences show angular to sub-rounded sedimentary clasts suspended within a sulphide (galena, sphalerite) and chlorite-garnet-quartz matrix (Figure 15C). Albite, chlorite, sericite alteration and goethite/hematite mottling occur adjacent to the Ore Shoot Fault north of the mound deposit.

The thinly-bedded, varved siltstone unit shows pervasive biotite and sericite alteration and patchy tourmaline replacement. The alteration intensifies to the south eventually forming a 1.5 m thick unit of coarse white mica and magnesium-rich tremolite (Figure 16). Silicification, albitization, disseminated pyrrhotite, sericitic bleaching, and oxide mottling occur within the irregularly bedded quartz wacke and arenite that underlie these units.

Sampling

Twenty-four grab samples of various alteration types and lithologies were collected from the area (Table 7 and Figure 13). The highest values from the sampling were from sphalerite-rich, sericitic veinlets (SBA-2) showing 1988 ppm Zn and from galena-rich float boulders (SBA-1) at 64,400 ppm Pb. If these samples are excluded the average Pb value is 25.1 ppm while Zn averaged 79 ppm.

Interpretation

Fragmental rocks at SBA occur near the intersection of the northerly-trending Ore Shoot Fault and a series of northwest-trending structures and include an elliptical mound that is interpreted to be a vent-proximal deposit. The mound forms rounded outcrops of crudely-bedded fragmental material that are interpreted as an extrusive seafloor edifice built around a central conduit. Discordant fragmental rocks flanked by tilted and broken quartz wacke units that underlie the mound may represent the root zone of the unit.

Debris flows from the growing mud-volcano created proximal fragmental units during episodic sediment volcanism. Discordant fragmental breccias within the hanging wall of the mound indicate the system remained active after formation of the mound.

Intense hydrothermal alteration is best developed in the footwall of the mound deposit and includes pervasive sericite, biotite, and tourmaline alteration. Bedded tremolite/mica located in the footwall of the mound deposit along a distinctive varved horizon is interpreted to represent metamorphism of an originally vented carbonate unit. Low base metal values within the R and Shaft mudstone, flanking the fragmental units, imply the system was not actively venting and depositing base metals during sedimentation. The garnet-rich massive sulphide float boulders discovered in the vicinity of the fragmental unit likely indicate a mineralized zone within the larger system.

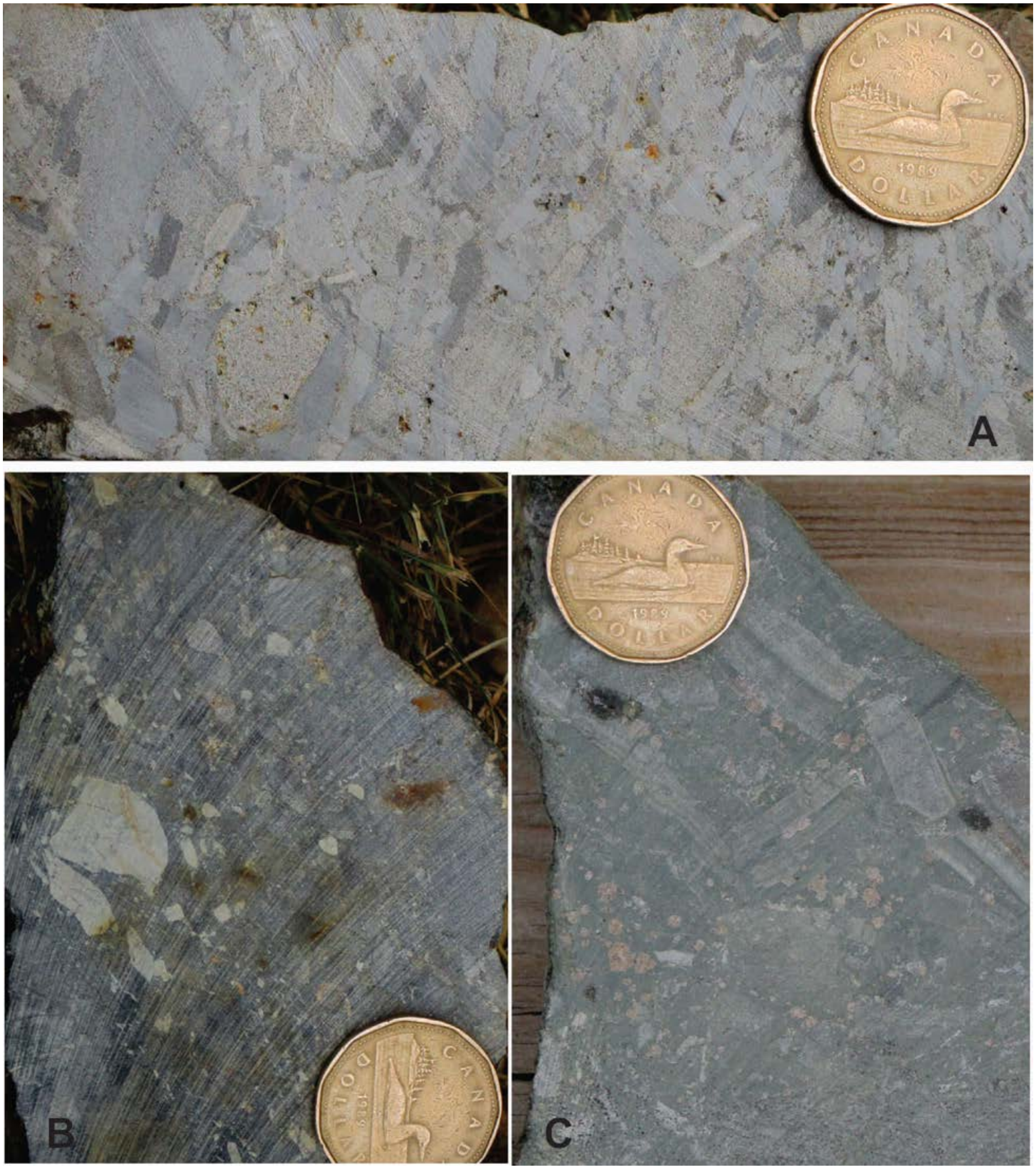

Figure 15. *Fragmental rocks from SBA. A) Polylithic mound deposit fragmental unit, note clasts define an approximate bedding. B) Discordant sedimentary breccia, white albitic (?) clasts in a dark silty matrix show a preferred orientation along an inferred fluidization path. C) Discordant sedimentary breccia with chlorite and garnet rich matrix.*

Figure 16. *Bedded exhalitive carbonate unit (calcite, tremolite, white mica).*

Table 7. *Geochemical analyses from the SBA.*

Sample	Mo	Cu	Pb	Zn	Ag	Ni	Co	Mn	Fe	As	Au	Th	Sr	Cd	Sb	Bi	V	Ca
	PPM	PPM	PPM	PPM	PPM	PPM	PPM	PPM	%	PPM	PPB	PPM	PPM	PPM	PPM	PPM	PPM	%
SBA 1	0.2	75.5	64400.0	298	133.0	2.2	2.5	1279	5.96	2.1	17.2	4.4	2	8.4	152.3	0.5	14	0.09
SBA-2	3.2	23.7	34.4	1988	0.2	11.8	7.6	628	3.73	1.0	0.5	11.1	6	5.4	0.4	1.0	38	0.20
SBA-3	0.6	25.5	16.5	40	0.1	2.8	2.2	194	2.38	0.5	0.5	10.2	14	0.1	0.2	0.4	22	0.05
SBA 4	4.7	2.5	42.6	250	0.1	36.2	15.4	1296	5.11	0.5	0.5	14.4	4	0.1	0.2	0.1	85	0.19
SBA-5	0.2	0.9	1.8	10	0.1	2.7	0.4	32	0.28	0.5	0.8	11.0	2	0.1	0.1	0.6	4	0.08
SBA 6	0.5	78.4	66.6	5	0.1	10.0	7.0	49	1.81	12.4	0.5	17.1	3	0.1	0.6	2.3	3	0.01
SBA-7	0.9	12.5	7.1	50	0.1	10.2	6.6	445	3.63	6.4	2.0	11.6	14	0.1	0.2	3.5	53	0.09
SBA 8	1.4	26.9	17.8	100	0.1	24.7	9.7	697	2.93	0.5	0.5	9.9	27	0.1	0.3	0.9	58	0.45
SBA-9	0.7	1.5	3.1	29	0.1	24.1	8.5	242	2.51	19.3	3.4	10.9	4	0.1	0.6	3.2	24	0.12
SBA-10	0.3	0.5	3.9	8	0.1	17.6	6.8	85	0.41	15.6	1.7	9.6	4	0.1	0.2	2.0	7	0.14
SBA-11	4.8	34.8	16.8	98	0.1	29.8	12.6	310	3.61	0.6	0.5	11.5	40	0.2	0.4	0.4	36	0.64
SBA-12	1.2	27.9	22.2	91	0.1	23.9	11.0	498	3.19	0.5	1.5	8.6	64	0.2	0.2	0.3	50	1.27
SBA-13	1.2	30.9	25.9	109	0.1	28.1	13.7	447	3.41	0.5	0.5	10.3	80	0.2	0.1	0.5	51	1.77
SBA-14	5.2	23.1	199.6	40	0.3	2.3	1.2	460	4.42	0.9	0.5	10.6	15	0.1	0.2	1.0	20	0.13
SBA-15	4.6	39.3	15.8	38	0.1	27.1	11.9	487	3.53	1.3	0.8	10.4	14	0.2	0.7	0.3	18	0.39
SBA-16	3.0	37.3	19.8	97	0.1	26.2	11.2	455	3.13	0.5	0.5	10.9	16	0.4	0.4	0.4	28	0.35
SBA-17	0.4	11.1	10.8	29	0.1	2.8	2.0	169	1.82	0.6	1.3	12.2	7	0.1	0.2	0.4	12	0.03
SBA-18	0.7	12.9	12.3	64	0.1	7.1	4.4	244	2.73	4.6	0.9	13.8	27	0.1	0.2	0.4	20	0.02
SBA-19	0.7	16.2	16.2	51	0.1	13.6	8.4	227	2.20	4.5	0.5	12.2	9	0.1	0.2	0.4	14	0.08
SBA-20	8.4	40.1	24.4	121	0.1	31.9	12.6	476	3.73	0.5	0.5	12.3	13	0.1	0.4	0.5	40	0.28
SBA-21	0.5	17.1	10.1	306	0.1	12.6	7.5	265	2.17	7.8	0.5	11.9	6	0.4	0.3	0.2	12	0.09
SBA-22	0.9	18.0	11.1	79	0.1	15.2	8.0	152	1.67	0.5	0.5	10.2	4	0.1	0.2	0.3	10	0.07
SBA-23	0.2	31.6	3.5	49	0.1	39.6	12.1	904	5.01	0.7	0.5	12.7	11	0.1	0.2	0.2	68	0.17
SBA-24	0.6	4.4	4.2	67	0.1	2.5	18.8	1351	7.27	0.7	0.5	2.1	196	0.1	0.3	0.2	75	1.36

Sample	P	La	Cr	Mg	Ba	Ti	B	Al	Na	K	W	Hg	Sc	Tl	S	Ga	Se	Te
	%	PPM	PPM	%	PPM	%	PPM	%	%	%	PPM	PPM	PPM	PPM	%	PPM	PPM	PPM
SBA 1	0.006	15	10	0.40	4	0.024	1	1.76	0.002	0.04	0.1	0.01	2.2	0.1	1.32	5	0.5	0.2
SBA-2	0.047	33	33	1.54	39	0.096	1	1.89	0.091	0.21	0.1	0.02	4.1	0.2	0.77	7	0.8	0.2
SBA-3	0.015	11	17	0.56	111	0.097	2	1.26	0.049	0.87	0.1	0.01	3.3	0.6	0.19	4	0.5	0.2
SBA 4	0.047	11	56	10.32	262	0.310	1	8.54	0.037	6.80	0.1	0.01	7.9	3.2	0.05	24	0.5	0.2
SBA-5	0.042	11	4	0.16	73	0.009	1	0.81	0.020	0.45	0.1	0.01	0.8	0.1	0.05	1	0.5	0.2
SBA 6	0.014	35	4	0.07	30	0.025	1	0.33	0.013	0.19	0.1	0.01	0.8	0.1	1.32	1	4.2	0.2
SBA-7	0.046	45	44	3.25	100	0.222	1	3.64	0.047	2.60	0.1	0.01	6.6	1.8	0.05	14	1.3	0.2
SBA 8	0.053	27	47	3.27	101	0.156	1	3.82	0.163	1.72	0.1	0.01	11.0	0.9	0.29	13	2.6	0.2
SBA-9	0.051	22	22	2.18	78	0.129	3	2.65	0.025	1.54	0.1	0.01	2.7	1.0	0.05	7	0.5	0.3
SBA-10	0.056	19	7	0.36	50	0.018	2	0.87	0.016	0.52	0.1	0.01	1.2	0.2	0.05	2	0.5	0.2
SBA-11	0.069	29	28	1.70	138	0.193	1	2.90	0.187	1.73	0.1	0.01	3.8	0.9	0.91	8	0.5	0.3
SBA-12	0.060	21	39	1.60	89	0.176	1	3.75	0.366	1.63	0.1	0.01	7.0	0.8	0.64	12	0.6	0.2
SBA-13	0.055	23	40	1.69	79	0.207	1	4.32	0.409	1.78	0.1	0.01	7.6	0.9	0.74	12	0.5	0.2
SBA-14	0.068	41	26	1.11	38	0.122	1	1.46	0.054	0.23	0.1	0.01	1.9	0.1	0.09	5	0.9	0.2
SBA-15	0.058	37	22	1.00	51	0.121	1	1.29	0.047	0.37	0.1	0.01	1.7	0.3	1.09	4	0.5	0.2
SBA-16	0.067	39	26	1.26	140	0.148	1	1.89	0.082	1.31	0.1	0.01	2.3	0.8	0.85	5	0.6	0.2
SBA-17	0.026	13	12	0.55	103	0.088	1	1.18	0.026	0.88	0.1	0.01	1.6	0.6	0.11	3	0.5	0.2
SBA-18	0.032	42	17	0.67	127	0.130	1	1.72	0.024	1.15	0.1	0.01	2.2	0.8	0.12	5	0.5	0.2
SBA-19	0.022	40	13	0.44	113	0.109	1	1.13	0.038	0.83	0.1	0.01	1.7	0.6	0.22	3	0.5	0.2
SBA-20	0.067	59	35	1.51	151	0.177	1	2.14	0.078	1.55	0.1	0.01	4.0	1.0	0.91	8	0.7	0.2
SBA-21	0.023	49	13	0.51	75	0.043	1	1.05	0.036	0.35	0.1	0.01	1.6	0.2	0.27	4	0.5	0.2
SBA-22	0.020	5	11	0.55	72	0.084	1	1.02	0.030	0.73	0.1	0.01	1.5	0.4	0.41	3	0.5	0.2
SBA-23	0.033	32	42	1.29	68	0.082	1	2.37	0.049	0.19	0.1	0.01	7.1	0.1	0.05	14	0.5	0.2
SBA-24	0.425	28	1	1.78	56	0.130	1	2.98	0.045	0.13	0.1	0.01	1.5	0.1	0.05	11	0.5	0.2

SBA-1 (discordant fragmental; chlorite, garnet, actinolite, galena), SBA-2 (siltstone, quartz wacke, fracture sphalerite), SBA-3 (debris flow), SBA-4 (bedded white mica and tremolite horizon), SBA-5 (vent proximal mound; sericitic) SBA-6 (quartzite, serecite), SBA-7 (debris flow), SBA-8 (debrs flow; biotite, pryhhotite), SBA-9, 10 (varved siltstone; sericite), SBA-11-13 (siltstone, quartz wacke; calcareous, pyrrhotite), SBA -14,15 (siltstone, quartz wacke; calcareous, pyrrhotite), SBA-16 (argillite; pyrrhotite), SBA-17,18 (vent proximal fragmental), SBA-19 (vent proximal fragmental; phlogopite), SBA -20 (argillite; calcareous), SBA-21 (vent proximal fragmental; silicified, pyrrhotite, sphalerite), SBA-22 (vent proximal fragmental; silicified, sericitized), SBA-23 (discordant fragmental; chlorite, silicified), SBA-24 (gabbro; quartz-chlorite veins)

VINE WEST

The Vine West is centered at UTM 584,000mE and 5,473,700mN (Figure 1) approximately 14 km south-southwest of Cranbrook. The area is accessed by a network of old logging roads south of the Peavine Creek Forest Service Road, off Highway 3 approximately 7 km south of Cranbrook. Fragmental rocks crop out along a steep hillside located immediately above Highway 3. Elevation in the area of fragmental rocks ranges from 1100 to 1300 m. The steep slopes above Highway 3 are generally grassy and contain abundant outcrop while the top of the hill plateaus into a forested area with poor exposure.

Geology

The area is bound to the south by the northeast striking, northwest dipping Moyie reverse fault (Brown et al., 2011a). A series of northwest-trending faults, including the Vine Fault, dissect the area north of the Moyie Fault. Bedding in the immediate area of the Vine West strikes southwest and dips shallowly to the northwest. Stratigraphically the Vine West is bracketed by the Sundown and Meadowbrook sills (see Figure 3).

History

The Vine West area is located along the northwest extension of the Vine Fault which hosts the Vine massive sulphide vein deposit 2.5 km to the southeast. The Vine vein was discovered by D. Pighin in 1976. It is a steeply-dipping northwest-trending massive sulphide vein related to a gabbro dyke that cuts Lower and Middle Aldridge wacke and siltstone with proven reserves of 240,000 tonnes at 5.2% Pb, 2.24% Zn, 67.23 g/t Ag and 1.92 g/t Au (Höy et al., 1995). Geochemical and geophysical surveys and limited trenching conducted along the extension of the Vine Fault in the Vine West area were carried out in the early 1990s by Kokanee Explorations Ltd (Höy et al., 1995). The area is currently being explored for massive sulphide potential by PJX Resources.

Description of Fragmental Units

The Vine West area is underlain by thin to medium-bedded quartz wacke with significant intervals of rusty, pyrrhotitic, thinly bedded, calcareous siltstone, wacke, and lesser argillite. Bedded to discordant fragmental rocks occur along a greater than 400 m northwest trend and remain open along strike (Figure 17).

During mapping the fragmental rocks at Vine West were informally divided into lower and upper members. The lower fragmental unit is a clast- to matrix-rich, crudely-bedded conglomerate that crops out on a south-facing rounded hillside. It has a north-south trending elliptical geometry approximately 100 m long by 50 m wide. Clasts range from cm to dm in diameter, are polylithic (argillite, siltstone, quartzite), with ragged, tabular, and elliptical forms and show minimal sorting. The eastern edge of the unit is bound by a northerly-trending, steep east-dipping zone of cleavage and fracturing. The conglomeritic unit is overlain by irregularly bedded flinty argillite/siltstone and irregular mud/siltstone breccias. The capping argillite/siltstone unit can be traced to the west where it becomes a thin to medium-bedded, planar-laminated, calcareous and sulphidic siltstone/wacke. West of this unit, and footwall to the upper fragmental package, is a thick sequence of medium to thickly-bedded quartz wacke. An approximately 35 m thick section of, thinly bedded argillaceous siltstones with variable sulphide content (Figure 18 A) occur in the

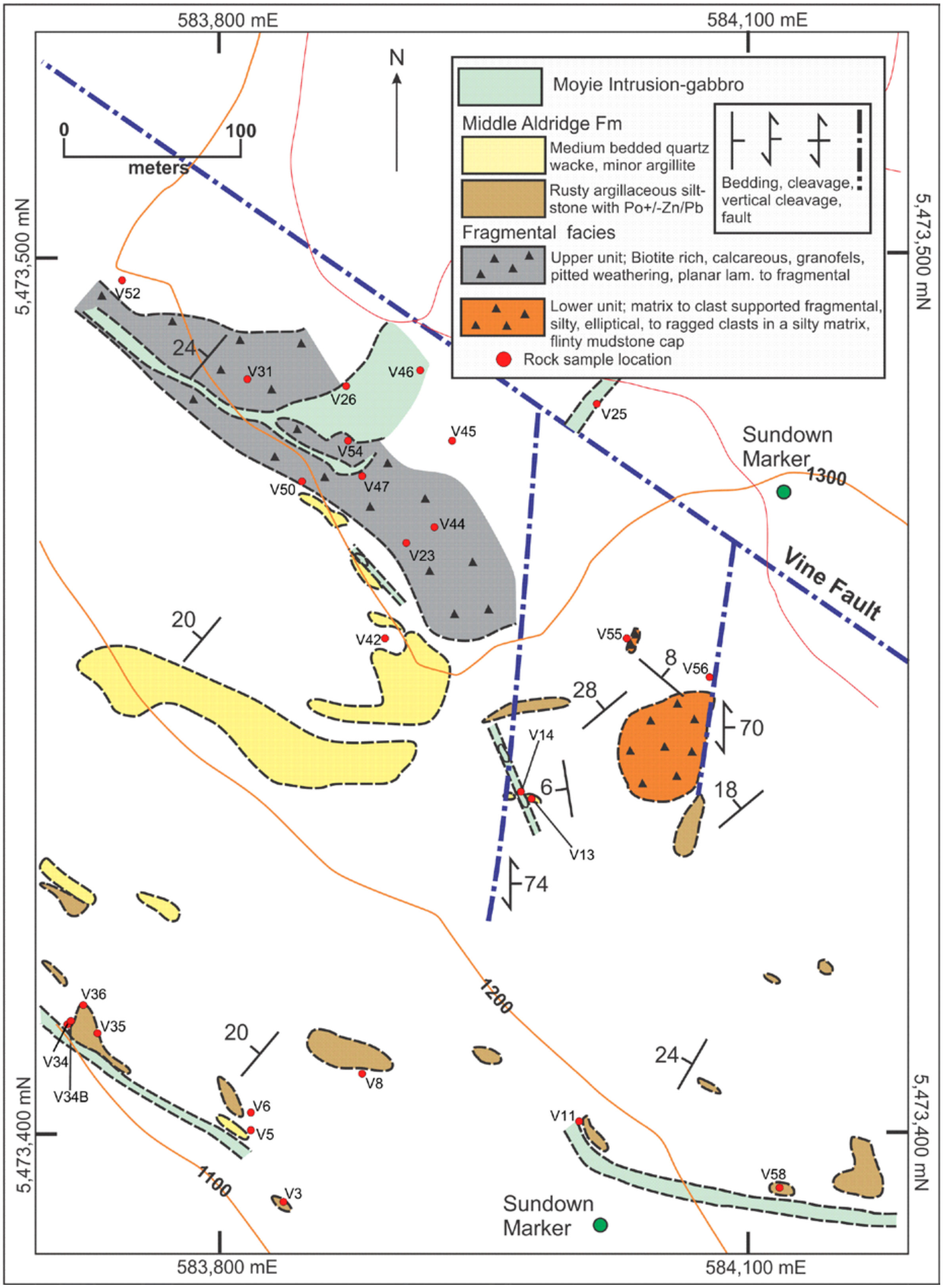

Figure 17. *Geology of the Vine West fragmental complex.*

Figure 18. *Photos of Vine West fragmental units. A) Thin-bedded sphalerite-bearing siltstone from the lower geochemically active horizon. B) Biotite and calcite rich fragmental rock from the upper fragmental unit (Vine West)*

footwall of the fragmental unit above a narrow (less than 10 m wide), irregular phaneritic, chlorite-, biotite-, and quartz-rich diorite sill.

The upper fragmental is comprised of massive beds showing slumping or rip-up clasts, and angular clast-rich conglomerates intercalated within a sequence of biotite-rich, calcareous, thin-bedded and rusty, quartzite, argillaceous siltstone, and lesser medium-bedded quartz wacke (Figure 18 B). The thickness of the entire upper package varies from approximately 25-30 m in the northwest to approximately 75 m proximal to a northerly-trending fault. It is exposed for nearly 300 m and remains open to the northwest and northeast. Clasts within fragmented rocks in the upper unit range from mm- to m-scale. Clast- to matrix-rich intensely biotite-altered, calcareous and sulphidic discordant fragmental breccias are seen to locally cut the bedded stratigraphy within the upper unit. Locally m-scale slabs of well-bedded siltstone and wacke have been incorporated into these cross-cutting breccias. In the field, the upper fragmental package has a dark, pitted to differentially weathered character showing a fine- to coarsely-grained biotite granofels texture that fizzes vigorously with dilute HCl. Calcite and biotite-rich veins are common within the unit.

An irregular phaneritic sill composed of chlorite, biotite, and quartz, similar to the sill below the lower fragmental, intrudes the upper fragmental package. The sill is generally massive but locally displays a linear fabric parallel to bedding. The sill contact is highly irregular, showing splays and pinch and swell structures and in places appears incorporated into the fragmental unit.

Structure

Bedding in the area typically strikes northeast with a shallow dip to the northwest. Above the lower fragmental unit bedding attitudes define an open, shallow north-plunging anticline. The major structural feature in the area is the normal, northwest-trending, Vine Fault which occurs immediately northeast of the fragmental units. Near the Vine vein the Vine Fault dips steeply to the west and has a dip-slip offset of approximately 80 m (Höy, 1995). A parallel north-northwest trending quartz-chlorite shear zone occupied by a narrow gabbro dyke was mapped during the project west of the projection of the Vine structure. This structure has localized some discordant fragmental rocks inferring the structure was active during basin development. At least two northerly-trending structures that are defined by zones of minor shearing with chlorite and quartz veining occur southwest of the Vine Fault. At least one of these structures appears to have been syn-depositional as reflected by the observed thickening of the upper fragmental package proximal to the fault and also the change in sedimentary facies observed in rocks on either side of the structure below the upper fragmental package. Irregular zones of northeast-striking and northwest-dipping shearing were observed above the lower diorite sill.

Mineralization and Alteration

Alteration within the lower fragmental unit includes patchy biotite, sericite, chlorite, albite and silicification. Sulphide mineralization includes pyrrhotite, rare chalcopyrite and sphalerite. Overlying the lower diorite sill, footwall to the lower fragmental unit, is an interval of biotitic, argillaceous siltstone with disseminated to stratabound pyrrhotite, galena, sphalerite.

The upper fragmental unit and interbedded sedimentary strata are intensely biotite-altered and calcite-rich (Figure 19 A). Sulphide mineralization comprising stringers, clots, and disseminations of chalcopyrite and pyrrhotite are best developed within cross-cutting breccias

(Figure 19 B) and proximal to the mafic dyke. Three polished thin sections from the upper fragmental package show a potassic feldspar alteration overprinting the unit (Figure 20).

Sampling

A total of 25 rock samples were collected from the Vine West and are results are shown in Table 8. The data appears to define two base metal intervals (see Figure 17). The lower interval is an approximately 35 m thick, thinly bedded argillaceous siltstone that crops out below the lower fragmental unit and contains elevated values of zinc, lead, manganese and vanadium. The other interval occurs in the upper fragmental biotite-rich unit and contains elevated values for copper, zinc, manganese and vanadium throughout.

Interpretation

At Vine West bedded to discordant fragmental rocks, interpreted as vent proximal debris flow and mound deposits, occur throughout approximately 200 m of stratigraphy along a greater than 400 m northwest trend. Fragmental units are localized at the intersection of north-south and northwest-trending syn-sedimentary structures.

The lower fragmental unit is interpreted as a debris flow conglomerate that has filled a local depression west of a northerly-trending syn-depositional fault. This unit is overlain by irregularly bedded flinty sedimentary strata and mudstone/siltstone breccias that may have originated as a pulse of liquefied mud-rich material ejected from a local vent.

The intensely biotite altered, calcareous, upper fragmental package is interpreted as a mound deposit that formed within in an active hydrothermal system. The package thickens proximal to a northerly-trending fault. An irregularly defined diorite dyke is locally incorporated into the fragmental/sedimentary unit indicating injection into the mound during sedimentation, and high heat flow. Discordant fragmental rocks within the upper package are localized along a northwest-trending structure that appears to bound the unit to the west. Alteration and sulphide mineralization increases within these discordant units indicating that they were a focus for mineralizing fluid flow.

Geochemically anomalous rock samples from footwall rocks and the upper fragmental unit may indicate that the area was actively venting sulphide rich fluids during sedimentation. Highly anomalous values for vanadium (up to 658 ppm) may indicate euxinic conditions during sedimentation (Breit et al., 1989).

.

Figure 19. *Field photos from Vine West. A) Calcite and biotite-rich thinly bedded siltstone and conglomerate (Vine West). B) Biotite altered quartz wacke clasts in a silty-biotite/pyrrhotite rich matrix (Vine West)*

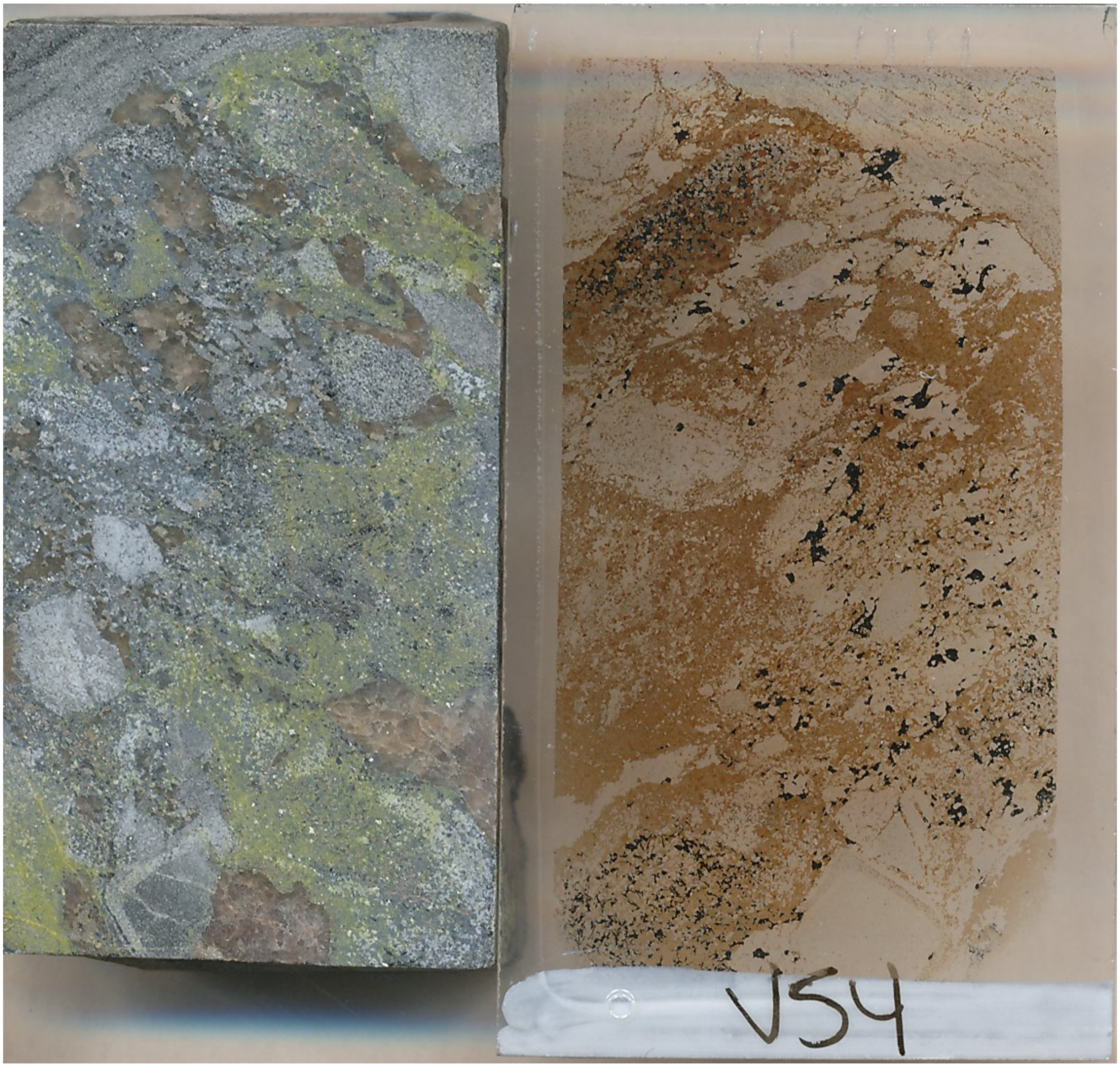

Figure 20. *Polymict fragmental rock from Vine West with quartz, biotite, clinozoisite, albite, and white mica matrix overprinted by a later hydrothermal event (K-feldspar, dolomite/calcite, white mica, pyrrhotite, pyrite and clay).*

	Mo	Cu	Pb	Zn	Ag	Ni	Co	Mn	Fe	As	Au	Th	Sr	Cd	Sb	Bi	V	Ca
Sample	PPM	PPM	PPM	PPM	PPM	PPM	PPM	PPM	%	PPM	PPB	PPM	PPM	PPM	PPM	PPM	PPM	%
V3	0.4	87.4	7.9	174	0.1	52.6	21.3	1022	8.06	14.8	4.3	2.2	20	0.1	0.1	0.2	315	0.27
V5	3.4	25.2	23	296	0.1	26.2	12.1	496	2.76	1.4	0.5	10.9	19	0.6	0.3	0.1	28	0.33
V6	0.4	26.4	22.3	114	0.1	20.2	8.8	820	2.81	3.4	0.5	9.9	78	0.2	0.3	0.1	35	2.05
V8	1.4	18.3	176	143	0.5	10.5	4.2	400	2.52	2.8	0.5	10.3	14	0.2	0.3	1.6	27	0.24
V11	0.2	92.7	7.2	135	0.1	62.4	41.2	1307	6.62	28.1	0.5	1.4	67	0.1	0.1	0.1	261	5.06
V13	2.3	45.1	3.3	34	0.1	24.6	9.9	473	3.68	22.6	0.5	10.3	5	0.1	0.3	0.1	38	0.22
V14	0.8	30.9	165.6	177	0.3	24.9	11.4	886	3.61	5.9	12.5	9.6	42	0.5	0.3	0.7	44	2.6
V23	0.3	143	10.8	137	0.1	52.3	33	1695	6.74	7.3	6.9	4.4	87	0.2	0.1	0.3	219	2.42
V25	0.3	33.5	17	126	0.1	72.3	35.9	2105	5.84	54.4	4.6	1.7	203	0.1	0.2	0.2	422	3.92
V26	0.1	166.3	13.3	90	0.2	61.7	36.1	661	4.63	21.1	2.4	1.2	105	0.2	0.1	0.1	175	3.54
V31	1.3	94.5	16.6	124	0.1	32.1	49.3	514	7.29	367.9	12.9	1.4	133	0.1	0.3	0.4	658	2.98
V34	1.8	77.1	35	67	0.2	11.3	11.4	407	2.31	5.6	0.5	9.3	9	0.1	0.2	0.3	30	0.21
V34B	3.5	13.4	84.3	31	0.2	2.8	1.7	616	2.56	5	0.5	10.8	5	0.1	0.7	0.3	30	0.14
V35	2.3	52.7	32.2	93	0.1	10.3	7	460	2.82	3.1	0.5	10	13	0.1	0.3	0.3	29	0.17
V36	0.6	23.6	163.6	122	0.3	14.3	8.4	668	3.24	1.8	2.5	9.7	18	0.2	0.4	0.5	34	0.45
V42	0.1	27.4	6	36	0.1	4.8	2.7	157	1.88	7	0.5	11.2	8	0.1	0.2	0.2	13	0.06
V44	1.0	73.3	12.2	44	<0.1	28.1	11.2	301	2.32	21.2	<0.5	6.8	9	<0.1	0.6	0.3	9	0.15
V45	1.9	24.4	19.5	194	0.1	22	9.9	1189	3.61	7.1	1.2	9.6	70	0.4	0.3	0.9	31	3.76
V46	0.7	267	10.3	142	0.1	67.9	62.5	940	10.33	92.7	22.1	1.6	95	0.1	0.1	0.9	543	2.26
V47	0.3	49.6	18.1	230	<0.1	59.4	45.1	2794	9.18	26.7	5.8	3.0	134	0.2	0.1	0.4	404	8.35
V50	0.2	68.5	9.8	20	0.1	5.8	5.3	117	1.44	11.3	1.1	7.3	28	0.1	0.1	0.1	9	0.41
V52	2.5	31	10.4	52	0.1	30.8	15.3	846	2.59	46.6	2.3	13.1	75	0.1	0.3	0.3	29	3.21
V54	0.4	230.0	12.0	139	0.1	51.1	37.3	1815	11.04	62.3	8.2	4.4	83	0.2	0.2	0.8	183	3.96
V55	0.5	24.3	8.1	49	0.1	18.8	9.5	283	3.09	27.4	0.5	14.3	16	0.1	0.2	0.1	21	0.2
V56	1.4	20.3	27.7	218	0.1	25.5	19.5	313	2.21	141.3	0.5	10.7	38	0.2	0.5	0.1	18	0.38
V56B	0.2	1.2	5.6	9	0.1	3.6	4.4	107	0.37	16.4	0.5	19.1	5	0.1	0.2	0.1	3	0.14
V58	1.5	27.8	257.8	225	0.5	21.1	10.8	551	3.21	0.6	1.5	10.1	21	1.3	0.5	0.8	31	0.48

	P	La	Cr	Mg	Ba	Ti	B	Al	Na	K	W	Hg	Sc	Tl	S	Ga	Se	Te
Sample	%	PPM	PPM	%	PPM	%	PPM	%	%	%	PPM	PPM	PPM	PPM	%	PPM	PPM	PPM
V3	0.035	3	198	3.19	670	0.488	1	5.23	0.077	3.97	0.1	0.01	45.4	1.7	0.19	17	0.5	0.2
V5	0.066	16	25	1.53	120	0.157	1	2.06	0.069	1.45	0.1	0.01	3	0.8	0.59	6	0.5	0.2
V6	0.053	20	37	1.9	112	0.182	1	2.67	0.124	1.72	0.1	0.01	3.6	0.8	0.06	8	0.5	0.2
V8	0.053	18	30	1.01	65	0.15	1	1.58	0.065	0.55	0.1	0.01	3.9	0.3	0.05	5	0.5	0.2
V11	0.026	2	126	3.36	407	0.384	1	4.97	0.081	3.4	0.1	0.01	32.5	1.3	0.19	12	0.5	0.2
V13	0.022	24	28	0.93	28	0.104	1	1.73	0.033	0.15	0.2	0.01	4.8	0.1	0.05	8	0.5	0.2
V14	0.053	16	39	2.06	156	0.213	1	2.91	0.102	1.89	0.3	0.01	5.9	0.8	0.53	9	0.5	0.2
V23	0.069	7	71	1.78	302	0.333	1	5.48	0.129	2.49	0.1	0.01	18	1.3	0.05	14	1.5	0.2
V25	0.047	3	119	1.63	358	0.307	1	6.89	0.331	2.57	0.1	0.01	40.5	1.1	0.05	18	0.5	0.2
V26	0.031	4	130	2.83	295	0.202	1	5.75	0.183	1.66	0.1	0.01	9.2	0.6	0.05	11	0.5	0.2
V31	0.081	2	14	1.27	312	0.312	1	8.12	0.408	2.61	0.2	0.01	49.3	1.5	0.55	19	0.9	0.2
V34	0.048	10	24	1.17	133	0.177	1	1.64	0.04	1.24	0.1	0.01	3.4	0.6	0.37	6	0.5	0.2
V34B	0.045	12	27	1.49	32	0.122	1	1.7	0.031	0.18	0.1	0.01	3.6	0.1	0.07	9	0.5	0.2
V35	0.059	14	26	1.41	126	0.18	1	1.86	0.046	1.45	0.2	0.01	4.6	0.7	0.38	6	0.5	0.2
V36	0.054	17	32	1.75	164	0.2	1	2.36	0.09	1.64	0.1	0.01	4.8	1	0.39	8	0.5	0.2
V42	0.02	16	12	0.51	66	0.107	1	1.18	0.021	0.84	0.1	0.01	1.8	0.6	0.06	3	0.5	0.2
V44	0.025	15	8	0.32	44	0.047	<1	0.89	0.005	0.23	0.1	<0.01	1.2	<0.1	<0.05	3	<0.5	<0.2
V45	0.052	13	28	1.94	82	0.186	1	3.57	0.065	1.82	0.1	0.01	3	1.3	0.33	8	0.5	0.2
V46	0.074	4	11	1.84	106	0.344	1	6.14	0.319	2.86	0.2	0.01	41.6	1.5	1.19	18	1.4	0.2
V47	0.060	5	117	3.37	442	0.529	<1	8.09	0.150	4.23	0.1	<0.01	43.5	2.2	<0.05	21	<0.5	<0.2
V50	0.01	7	9	0.19	27	0.055	1	1.07	0.11	0.26	0.1	0.01	1.4	0.2	0.29	2	0.5	0.2
V52	0.041	16	27	1.21	140	0.181	1	4.3	0.124	1.48	0.1	0.01	3.9	0.7	0.05	9	0.5	0.2
V54	0.031	6	64	1.15	127	0.347	<1	5.08	0.166	2.62	0.1	<0.01	17.0	1.6	1.81	13	2.0	<0.2
V55	0.038	18	18	0.73	81	0.156	1	1.76	0.044	1.15	0.1	0.01	2.4	0.9	0.19	5	0.8	0.2
V56	0.04	12	17	0.98	56	0.129	1	1.93	0.112	1.01	0.1	0.01	2.1	0.6	0.29	5	0.5	0.2
V56B	0.049	16	3	0.04	45	0.055	1	0.48	0.022	0.25	0.2	0.01	1.1	0.1	0.05	1	0.5	0.2
V58	0.057	18	27	1.64	135	0.18	1	2.36	0.106	1.63	0.1	0.01	5	0.9	0.63	8	0.5	0.2

V3,5,6 (laminated siltstone), V8 (thin bedded siltstone, quartz wacke; albite), V11 (sediment-gabbro contact; biotite, albite, chlorite), V13 (thin bedded quartz wacke cut by chlorite breccia), V14 (gabbro dyke; quartz-carbonate veins), V23 (upper fragmental; granofels, calcareous), V25 (gabbro; granofels), V26,31 (upper fragmental; granofels, calcareous), V34 (thin bedded siltstone, quartz wacke; biotite), V34B (sheared thin bedded siltstone, quartz wacke; biotite), V35 (thin bedded siltstone; sericite, chlorite), V36 (thin bedded quartzite; disseminated galena, sphalerite), V42 (quartzite; sericite), V44 (upper fragmental; granofels, calcareous, quartz vein), V45 (argillite; pyrrhotite), V46,47 (upper fragmental; granofels), V50 (quartzite; sericite, albite, biotite), V52 (argillite; calcareous), V54 (upper fragmental; granofels), V55 (fragmental; silicified), V56 (fragmental; sericite, albite), V56B (fragmental; sheared, sericite), V58 (laminated siltstone; galena, sphalerite, magnetite)

Table 8*. Geochemical analyses from the Vine West*

Discussion

Structural and Lithological Implications

Fragmental rock units are localized along syn-depositional, rift-parallel faults and at the intersection of rift-parallel and syn-depositional transverse faults. Rift-parallel faults are often oriented north-northwest while transverse structures are oriented northeast (060˚) to east-west. As these structures generally show minimal to no apparent offset they are often difficult to define in the field (Figure 21). Minor changes in sedimentary facies and thickening of fragmental units are useful observations when defining these structures. Careful mapping of the geometry of fragmental units is an important tool in delineating controlling structures as they tend to have elongate outlines with a long axis parallel to early faults while discordant fragmental dykes may occupy said structures. Fragmental rocks have been shown to occur within anticlinal or synclinal structures where sediments have either overlapped vent proximal mounds, or have collapsed into depressions caused by extensional faulting, therefore detailed observations of bedding orientations (Figure 21) may help to define unexposed fragmental deposits. Mapping of debris flow deposits may likewise help define structures associated with mud volcanoes.

In the field fragmental rocks can be difficult to distinguish. Clasts are compositionally similar to the host Aldridge Formation and tend to be faded, generally not showing good textural contrast on a broken surface. However, the massive to rounded weathering nature of fragmental outcrops contrasts sharply to the well-bedded, tabular, nature of typical Aldridge Formation sedimentary rocks and is a useful tool for identifying fragmental units in the field.

Unique sedimentary units (rock units which are distinct from typical Aldridge Formation rocks) associated with fragmental units may represent important vectors for mineralization. Distinctly varved, thinly bedded siltstone-wacke units have been intensely altered at the Rise and SBA areas while biotite and calcite-rich thinly bedded units at Vine West contain anomalous geochemical values for base metals. Geochemical variations within certain horizons may define the broader areas influenced by exhalative plumes or hydrothermally altered cells. These units may also represent potentially replaceable host rocks.

Geochemistry

Geochemistry may be a useful and cost effective tool for vectoring within shallowly buried mud-volcano systems. The majority of geochemical data was collected from North Star (13 samples), SBA (23 samples), and Vine West (25 samples). Sampling at Rise, Ryder, and Pakk is limited in number and therefore not discussed here. A comparison of the geochemical values between the three sites is shown below (Table 9).

Based on the data set North Star shows higher than background values for As, Cu, Pb, and Zn. SBA shows higher than background values for only Zn, however this number is skewed due to sample SBA 2, 1988 ppm Zn. If this sample is omitted from the data set the Zn value drops to 79 ppm. The Vine West data set shows the highest values for Cu, Ni, Co, As, V, and Cr between the three areas.

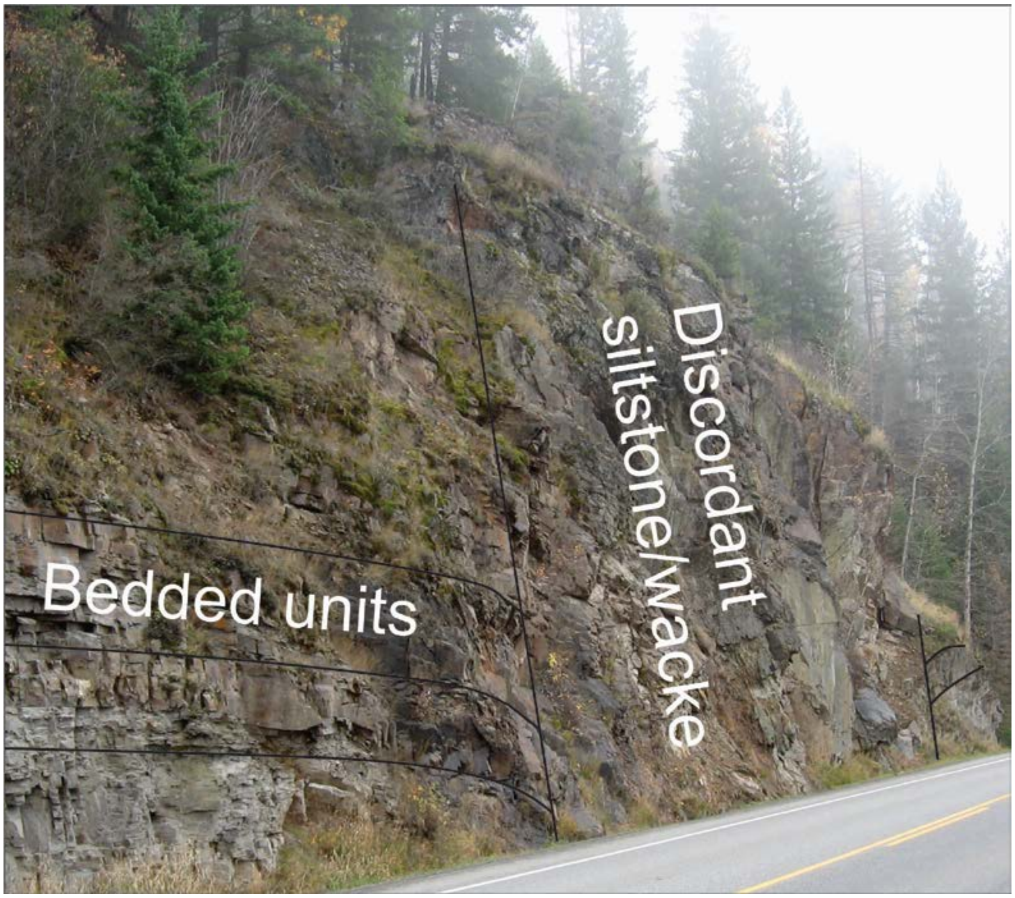

Figure 21. *Zone of discordant siltstone and wacke fragmental rocks 2 km south of the village of Moyie, BC. Note how the bedded units dip into the discordant zone and have no apparent offset on either side of the fragmental unit.*

Table 9. *Geochemical comparison of North Star with SBA and Vine West.*

Sample	Cu	Pb	Zn	Ni	Co	As	Sb	Bi	V	Cr
	PPM	PPM	PPM	PPM	PPM	PPM	PPM	PPM	PPM	PPM
North Star	33.6	191.8	162	5.3	2.8	21.5	1.9	3.6	10	10
SBA	22.5	25.5	162	17.5	8.7	3.5	0.3	0.8	33	24
Vine West	69.8	36.5	119.5	31.7	20.4	39.5	0.26	0.38	144	49.5

Alteration

Alteration minerals, and their metamorphic derivatives, are key in locating ‘hot-spots’ within fragmental complexes. Systematic mapping of fragmental units and their host rocks may help define alteration patterns indicative of a focused zone of fluid upflow.

Previous workers have highlighted the importance of garnet as a vector for base metal mineralization within the Purcell Basin where the presence of garnet is an anomalous feature relative to the regional greenschist metamorphic grade (De Paoli et al., 2000, Pattison et al., 2011). Based entirely on observations during the 2014 mapping base metal mineralization within fragmental units is most closely associated with pervasive actinolite-biotite-chlorite-garnet-+/-albite+/-sericite alteration.

Conclusion

Fragmental rocks within the Aldridge Formation indicate areas where remobilized sediments have been transported along discordant feeder systems to extrude onto the sea floor to form mud volcanoes. These structures were important fluid flow pathways within the Purcell Basin, forming unique sedimentary environments and the plumbing systems for seafloor massive sulphide deposits, vent complex deposits, and later massive sulphide veins. Re-activation of these structures continued episodically and has been demonstrated to be associated with younger mineralizing events. They are an important feature for mineral exploration within the Purcell Basin.

While exploration in the Purcell Basin has focused mainly on the Lower-Middle Aldridge contact (Sullivan-time) our 2014 study has highlighted the potential of fragmental and mud-volcano systems in the Middle Aldridge. Fragmental rocks form along linear trends which effectively delineate structures which were active during sedimentation. Additional mapping and geochemistry is warranted to better define these structural trends and help define alteration/geochemical anomalies that may be associated with shallowly buried base metal systems.

Acknowledgements

We are greatly indebted to the tremendous amount of wisdom that has manifested itself around Sullivan over the course of its lifetime. Economic geologists, prospectors, and academic researchers who have helped unlock some of the mysteries of the Purcell Basin are too numerous to thank individually. We would like to thank Dave Pighin, Doug Anderson, Paul Ransom, Peter Klewchuk, Craig, Tom and Mike Kennedy, and Mike McCuaig for mentoring, and edits. Additionally we would like to thank industry partners who helped facilitate our program including Jim McDonald with Kootenay Silver Inc, and John Keating with PJX Resources Corp. A tremendous debt is owed to Elspeth Barnes for numerous edits, suggestions, motivation, and incredible patience. We would like to recognize and thank the late John W. Lydon for his pursuit and dedication to unravelling the Belt-Purcell. His mentorship, humbleness, encouragement and good humour will be greatly missed by all who knew him. Finally, we would like to thank and encourage all those who continue to believe in the Purcell Basin as we all recognize the next one will require equal parts good work, persistence, faith, and serendipity.

References

Anderson, D., (2006): Diamond drilling on the Pakk claims; *B.C. Ministry of Energy and Mines*, Assessment report 28424, 19 pages

Anderson, D., and Höy, T. (2000): Fragmental sedimentary rocks of the Aldridge Formation, Purcell Supergroup, British Columbia; *in the Geological Environment of the Sullivan deposit, British Columbia,* Geological Association of Canada, Special Publication 1, p. 261-271.

Breit, G. N., Wanty, R.W., Tuttle, M.L., (1989): Geochemical control on the abundance of vanadium in black shales and other carbonaceous rocks; *in Metalliferous Black Shales and Related Ore Deposits-Proceedings, 1989, United States Working Group Meeting, International Geological Correlation Program Project*, U.S. Geological Survey Circular 1058, p. 6-8.

Britton, J. M., Pighin, D. L., (1994): Fors – a Proterozoic sedimentary exhalative base metal deposit, Purcell Supergroup, southeastern British Columbia (82G/5W); *in* Geological Fieldwork 1994, Grant, B. and Newell, J. M., Editors, *B.C. Ministry of Energy, Mines and Petroleum Resources,* Paper 1995-1

Brown, D. A., Woodfill, R. D., (1998): The Moyie industrial partnership project: Geology and mineralization of the Yahk-Moyie Lake area, southeastern British Columbia (82F/01E, 82G/04W, 82F/08E, 82G/05W); *in* Geological Fieldwork 1997, *B.C. Ministry of Employment and Investment*, Paper 1998-1.

Brown, D.A. (1998): Geological Compilation of Grassy Mountain (East Half) and Moyie Lake (West Half) Map Areas, Southeastern British Columbia (82F/8E, 82G/5W); *B.C. Ministry of Energy and Mines, Geoscience Map 1998-3, 1:50 000 scale map.*

Brown, D.A., Macleod R.F., Wagner, C.L., and Chow, W (compilers), 2011a. Geology, Moyie Lake, British Columbia; Geological Survey of Canada, Open File 6303, scale 1:50,000. doi:10.4095/288545

Brown, D.A. and Macleod R.F. (compilers), 2011b. Geology, Yahk River, British Columbia; Geological Survey of Canada, Open File 6304, scale 1:50,000. doi:10.4095/288564

Brown, D.A., Macleod R.F., and Wagner, C.L. (compilers), 2011c. Geology, St. Mary Lake, British Columbia; Geological Survey of Canada, Open File 6308, scale 1:50,000. doi:10.4095/288567

Cook, F.A. and van der Velden, A.J. (1995) Three-dimensional crustal structure of the Purcell anticlinorium in the Cordillera of southwestern Canada; Geological Society of America, Bulletin, v.107, page 642-664.

Dimitrov, L.I., 2002: Mud volcanoes – the most important pathway for degassing deeply buried sediments. *Earth-Science Reviews 59*, 49-76

Gorton, M.P., Schandl, E.S., And Höy, T. (2000): Mineralogy and Geochemistry of Middle Proterozoic Moyie Sills, southern B.C.; *in the Geological Environment of the Sullivan deposit, British Columbia,* Geological Association of Canada, Special Publication 1, p. 322-335.

Höy, T. (1993): Geology of the Purcell Supergroup in the Fernie West-half map area, southeastern British Columbia; B.C. *Ministry of Energy and Mines*, Bulletin 84, 157 pages.

Höy, T., and Pighin, D.L. (1995): Vine – a Middle Proterozoic massive sulfide vein, Purcell Supergroup, southeastern British Columbia; *in* Geological Fieldwork 1994, Grant, B. and Newell, J. M., Editors, *B.C. Ministry of Energy, Mines and Petroleum Resources*, Paper 1995-1, p. 85-98.

Höy, T., Pighin, D. L., and Ransom P. W., (1994): Volcanism in the Middle Aldridge Formation, Purcell Supergroup, southeastern British Columbia; *in* Geological Fieldwork 1994, Grant, B. and Newell, J. M., Editors, *B.C. Ministry of Energy, Mines and Petroleum Resources*, Paper 1995-1, p. 73-83.

Jamtveit, B., Svensen, H., Poladchikov, Y. Y, Planke, S., 2004. Hydrothermal vent complexes associated with sill intrusions in sedimentary basins. *Breitkreuz, C., Petford, N., Editors. Physical Geology of High-Level Magmatic Systems. London, Geological Society of London, Special Publications*, 234, 233-241.

Kennedy, S. (2013): Report on geology, prospecting, rock and soil geochemistry; *B.C. Ministry of Energy and Mines*, Assessment report 34178, 50 pages.

Klewchuk, P. and Anderson, D., (1999): Diamond drilling on the Pakk claims; *B.C. Ministry of Energy and Mines*, Assessment report 26191, 60 pages.

Kopf, A.J., 2002: Significance of mud volcanism. *Reviews of Geophysics 40 (2).*

Lydon, J.W., 2007, Geology and metallogeny of the Belt-Purcell Basin, Goodfellow, W.D., ed., *in Mineral Deposits of Canada: A synthesis of Major Deposit-Types, District Metallogeny, the Evolution of Geological Provinces, and Exploration Methods:* Geological Association of Canada, Mineral Deposits Division, Special Publication No. 5, p. 581-607.

Lydon, J.W. (2008): Mineral deposits of Canada, District Metallogeny, SEDEX_Synopsis of the Belt-Purcell Basin: Geological Survey of Canada, http://gsc.nrcan.gc.ca/mindep/metallogeny/sedex/purcell/index_e.php

Lydon, J.W., Paakki, J.J., Anderson, H.E., and Reardon, N.C. (2000): Overview of the geology and geochemistry of the Sullivan deposit; *in the Geological Environment of the Sullivan deposit, British Columbia*, Geological Association of Canada, Special Publication 1, p. 505-522.

Pattison. D, Seitz, J. (2011). *Stabilization of garnet in metamorphosed altered turbidites near the St. Eugene lead–zinc deposit, southeastern British Columbia: Equilibrium and kinetic controls.* Lithos, March 2012, v. 134-135, p. 221-235.

Planke, S., Rasmussen, T., Rey, S.S., Myklebust, R. (2005). Seismic characteristics and distribution of volcanic intrusions and hydrothermal vent complexes in the Vøring and Møre basins. *In*: Doré, A.G., Vining, B.A. (editors) *Petroleum Geology: North-West Europe and Global Perspectives-Proceedings of the 6th Petroleum Geology Conference*, 833-844.

Planke, S., Svensen, H., Hovland, M., Banks, D. A., Jamtviet, B., 2003: Mud and fluid migration in active mud volcanoes in Azerbaijan. *Geo-Marine Letters 23*, 258-268

Ransom P.W., M.P., and Lydon, J.W. (2000): Geology, sedimentology, and evolution of the Sullivan sub-basin.; *in the Geological Environment of the Sullivan deposit, British Columbia*, Geological Association of Canada, Special Publication 1, p. 440-469.

Slack, J.F., Shaw, D.R., Leitch, C.H.B., and Turner, R.J.W. (2000): Tourmalinites and coticules: Geology, geochemistry and genesis; *in The Geological Environment of the Sullivan deposit, British Columbia*, Geological Association of Canada, Special Publication 1, p. 736-767.

Soloviev, S. (2009): Evaluation of 'Reduced' Intrusive-Related Gold Mineralization in the Area West of Cranbrook, Southeastern British Columbia (NTS 082F/49, 082F/50, 082F/59, 082F/60, 082G/41, 082G/51); in Geological Fieldwork 2009, *British Columbia Geological Survey*, Paper 2010-1, p. 97-111.

Svensen, H., Jamtveit, B., Planke, S., Chevallier, L., 2006. Structure and evolution of hydrothermal vent complexes in the Karoo Basin, South Africa. *Journal of the Geological Society*, 163, 671-682.

Svensen, H., Planke, S., Jamtveit, B., Pedersen, T., 2003: Seep carbonate formation controlled by hydrothermal vent complexes: a case study from the Vøring Basin, the Norwegian Sea. *Geo-Marine Letters 23*, 351-358

Turner, R,J.W., Leitch, C.H.B., Höy, T., Ransom, P.W., Hagen, A. And Delaney, G.D. (2000)A: Sullivan graben system: district setting of the Sullivan deposit; *in The Geological Environment of the Sullivan deposit, British Columbia*, Geological Association of Canada, Special Publication 1, p. 370-407.

Turner, R,J.W., Leitch, C.H.B., Ross, K.V. and Höy, T., (2000)B: Distric-scale alteration associated with thee Sullivan deposit, British Columbia; *in The Geological Environment of the Sullivan deposit, British Columbia*, Geological Association of Canada, Special Publication 1, p. 408-439.

Walker, R. T., (1996): Assessment report on a diamond drill progam, Cruz property; *B.C. Ministry of Energy and Mines*, Assessment report 24401, 64 pages